Accepted for publication in *Advances in Structural Engineering*.
http://dx.doi.org/10.1177/1369433218804928

Imperfection sensitivity in cylindrical shells under uniform bending

O. Kunle Fajuyitan[1] & Adam J. Sadowski[2]

Department of Civil and Environmental Engineering, Imperial College London

Abstract

Efforts are ongoing to characterise a comprehensive resistance function for cylindrical shells under uniform bending, a ubiquitous structural system that finds application in load-bearing circular hollow sections, tubes, piles, pipelines, wind turbine support towers, chimneys and silos. A recent computational study by Rotter *et al*. (2014) demonstrated that nonlinear buckling of perfect elastic cylinders under bending is governed by four length-dependent domains – 'short', 'medium', 'transitional' and 'long' – depending on the relative influence of end boundary conditions and cross-section ovalisation. The study additionally transformed its resistance predictions into compact algebraic relationships for use as design equations within the recently-developed framework of Reference Resistance Design (RRD). This paper extends on the above to present a detailed computational investigation into the imperfection sensitivity of thin elastic cylindrical shells across the most important length domains, using automation to carry out the vast number of necessary finite element analyses.

Geometric imperfections in three forms – the classical linear buckling eigenmode, an imposed cross-section ovalisation, and a realistic manufacturing 'weld depression' defect – are applied to demonstrate that imperfection sensitivity is strongly length-dependent but significantly less severe than for the closely-related load case of cylinders under uniform axial compression. The axisymmetric weld depression almost always controls as the most deleterious imperfection. The data is processed computationally to offer an accurate yet conservative lower-bound algebraic design characterisation of imperfection sensitivity for use within the RRD framework. The outcomes are relevant to researchers and designers of large metal shells under bending and will appeal to computational enthusiasts who are encouraged to adopt the automation methodology described herein to explore other structural systems.

Keywords

Uniform bending, nonlinear buckling, finite element analysis, imperfection sensitivity, ovalisation in cylindrical shells, automation.

[1] PhD Candidate in Structural Engineering
[2] Senior Lecturer in Structural Engineering

1. Introduction

A thin-walled cylindrical shell is an optimised structural form that is able to support high loads with minimal material use (Thomspon & Hunt, 1984; Rotter, 2004; Chapelle & Bathe, 2010). Cylindrical shells frequently appear as tubular piles, circular hollow sections, wind turbine support towers and slender silos, as well as aerospace vehicles, where the dominant form of loading is global bending. The search for a full understanding of the mechanics governing the behaviour of perfect cylinders in bending extends back by almost a century (Brazier, 1927; Wood, 1958; Seide & Weingarten, 1961; Reissner, 1961; Stephens *et al.*, 1975; Aksel'rad & Emmerling, 1984; Tatting *et al.*, 1997; Karamanos, 2002; Guarracino, 2003), a consequence of an inherently nonlinear fundamental response caused by cross-sectional ovalisation. Despite this historical effort, the crucial influence of cylinder length and thickness on ovalisation was only recently explored and characterised by the parametric study of Rotter *et al.* (2014), an advance made possible only with modern finite element software.

Analytical and computational studies investigating the particularly detrimental imperfection sensitivity of cylindrical shells under uniform compression boast a history that is almost as long (Koiter, 1945; 1963; Calladine, 1983; Rotter, 2004; Rotter & Al-Lawati, 2016), however a similar effort has not yet been undertaken for imperfect cylinders under uniform bending. In simple stress design, it is often assumed that the imperfection sensitivity relationship for uniform bending may be taken to be the same as for uniform compression (EN 1993-1-6, 2007), a conservative choice but one for which no rigorous proof had long been forthcoming. The first direct evidence of this, known to the authors, is the computational work of Chen *et al.* (2008) who conducted a limited parametric study on elastic-plastic clamped cylinders with realistic weld depression imperfections. The authors' own study in Fajuyitan *et al.* (2015) also appears to have been the first to identify that the sensitivity of cylinders under bending to the classical linear eigenmode imperfection may be strongly length-dependent, a consequence of a complex interaction between imperfections and pre-buckling ovalisation. Also known is the work of Vasilikis *et al.* (2016), who validated a set of thirteen four-point bending tests of thick tubes with a selection of shell finite element models that included imperfections relevant to the spiral welding manufacturing process, including eigenmode dimples, girth weld misalignment and residual stresses. However, a systematic investigation and documentation of the sensitivity of cylinders under bending to multiple imperfection forms across a wide range of parameters does not appear to have ever been performed.

2. Scope of the study

The aim of this paper is to present a comprehensive assessment of the sensitivity of cylindrical shells under uniform bending to three distinct forms of geometric imperfection. Rotter *et al.* (2014) demonstrated that the cylinder length L is responsible for controlling the extent of pre-buckling ovalisation of perfect elastic cylinders with rigidly-circular clamped ends. When transformed into dimensionless parameters ω or Ω (Eq. 1), the length allows a categorisation of geometric nonlinearity for the perfect system into four distinct domains termed 'short', 'medium', 'transitional' and 'long' (Fig. 1) in a manner that is independent of the radius to thickness (r/t) ratio. This is in contrast with only three length domains for cylinders under uniform compression (Rotter, 2004), which do not include a 'transitional' domain as they do not undergo ovalisation. For consistency, the above four length domain categorisations are retained in this study of imperfection sensitivity.

$$\omega = \frac{L}{\sqrt{rt}} \text{ and } \Omega = \frac{L}{r}\sqrt{\frac{t}{r}} \qquad (1a,b)$$

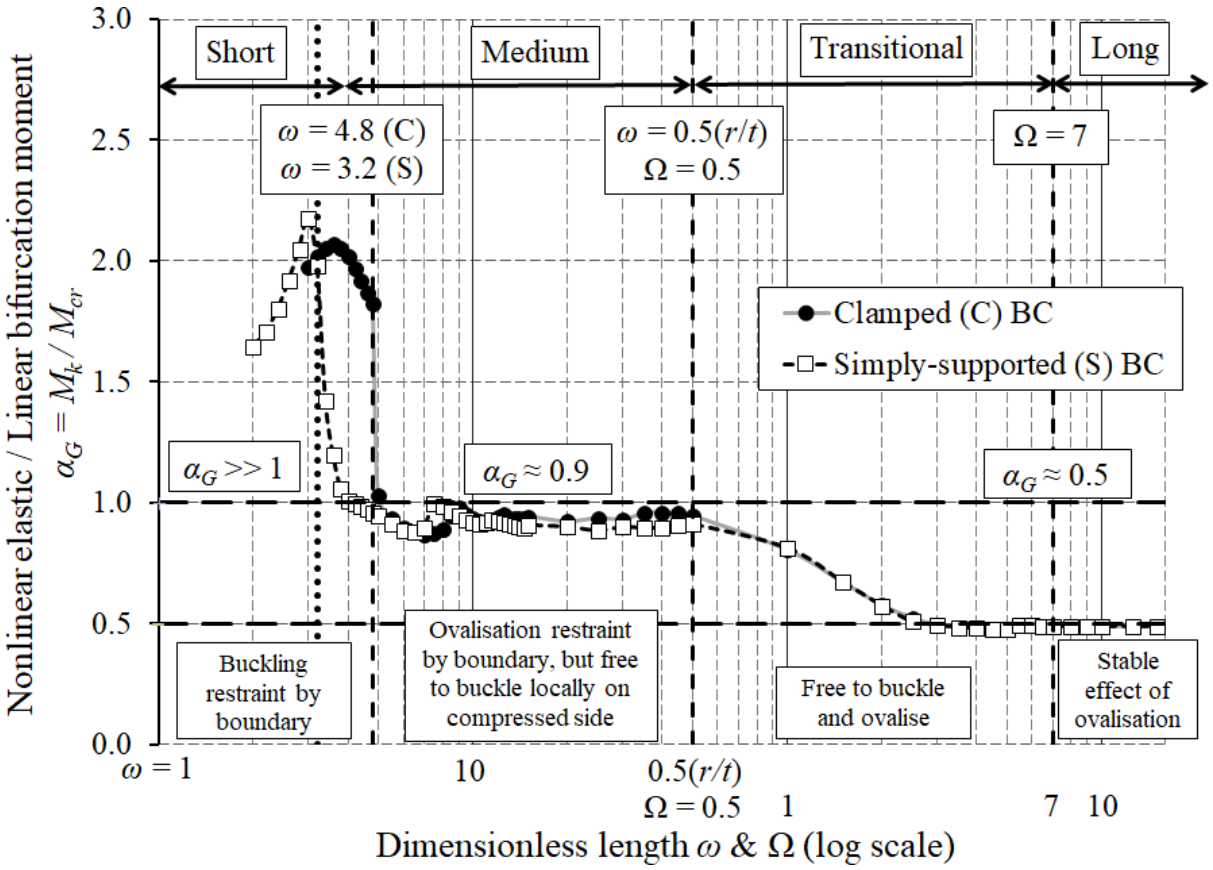

Fig. 1 – Length domains of geometrically nonlinear behaviour of cylinders under uniform bending (after Rotter *et al.*, 2014; Fajuyitan *et al.*, 2015).

The ‘short’ domain was the subject of two dedicated studies by Fajuyitan *et al.* (2017; 2018) and was found to exhibit either negligible or indeed beneficial imperfection sensitivity due to a pre-buckling stress state dominated by local compatibility bending with stable post-buckling behaviour. As rather few practical cylinders are truly ‘short’ (Rotter, 2004), this domain is perhaps of limited interest and cylinders shorter than $\omega = 5$ (approximately two linear bending half-wavelengths) are not considered further here. Similarly, the elastic behaviour of ‘long’ cylinders with fully-developed ovalisation is effectively invariant with further increases in length, and the upper limit of interest will be set at $\Omega = 10$. These bounds span several orders of magnitude of cylinder lengths and encompass all practical applications.

Three distinct forms of geometric imperfection with varying amplitude were investigated. The first is the classical critical linear buckling eigenmode, a staple of imperfection sensitivity studies in shells since the first asymptotic analyses of Koiter (1945; 1963) and presented as a ‘default’ imperfection form in computational analyses by the Eurocode on metal shells EN 1993-1-6 (2007). The second is an imposed initial ovalisation (in the form of circumferential harmonic two) to investigate the effect of bending on an already slightly flattened cylinder (Sadowski & Rotter, 2013a). The third is the axisymmetric circumferential ‘weld depression’ of Rotter and Teng (1989), a realistic representation of a manufacturing-related defect that has been widely used in computational studies of imperfection sensitivity in cylindrical shells (e.g. Song *et al.*, 2004; Sadowski & Rotter, 2011a). More details of each imperfection form are presented shortly.

The authors have chosen to contextualise the findings within the framework of Reference Resistance Design (RRD), recently developed by Rotter (2016a,b) as a method of manual dimensioning of shells based on resistances rather than working stresses and now accepted as a method of design through an Amendment to EN 1993-1-6 (Rotter, 2013). RRD is based around a ‘capacity curve’ functional form (Fig. 2) which relates a shell’s dimensionless characteristic resistance M_k / M_{pl}, where M_{pl} is the reference full plastic moment, to its dimensionless slenderness $\sqrt{(M_{pl} / M_{cr})}$, where M_{cr} is the reference elastic critical buckling moment. The continuous relationship is characterised by a set of dimensionless algebraic parameters, each accounting for a distinct physical phenomenon: geometric nonlinearity (α_G), imperfection sensitivity (α_I) and material nonlinearity (β, η, λ_0 and χ_h). In addition to now being an approved method of design, RRD offers a powerful research lens through which the nonlinearities governing a structural system may be established and understood in isolation.

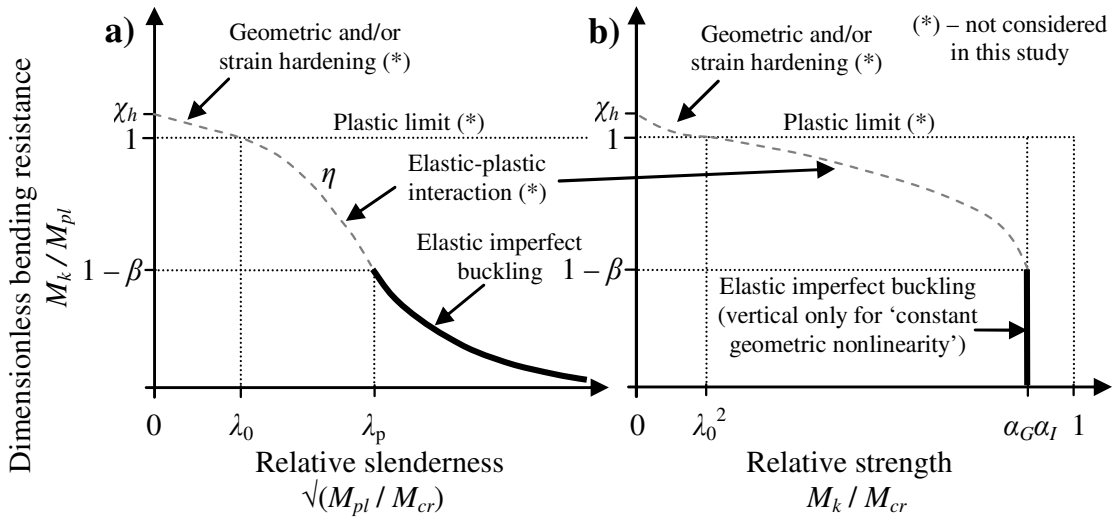

Fig. 2 – a) Generalised and b) Modified capacity curve functional form for cylinders under uniform bending (after Rotter, 2007). Only those nonlinearities relating to the elastic region (right-hand part of the curve, shown here as a thick line) are considered in this study.

A full characterisation of cylinders under bending within the RRD framework is part of a major ongoing research effort by the authors and will ultimately allow an analyst to predict the nonlinear bending resistance of a cylinder accurately and conservatively without recourse to an onerous finite element analysis. However, due to the vast number of parametric finite element analyses that are necessary to be performed, interpreted and processed to establish each RRD parameter (Sadowski *et al.*, 2017), it is not possible to present all findings within a single publication. The study of Rotter *et al.* (2014) on elastic perfect cylinders established α_G (Fig. 1), while the current paper on elastic imperfect cylinders aims to establish α_I. The plasticity-related parameters β, λ_0, η and χ_h are the focus of a separate dedicated study, currently in preparation (Wang *et al.*, 2018).

3. Computational methodology

3.1. Finite element model

The commercial ABAQUS v. 6.14-2 (2014) finite element software was used in this study. Each individual finite element model followed a quarter-shell design similar to those used in the authors' previous studies on cylinders under uniform bending (Chen *et al.*, 2008; Sadowski & Rotter, 2011a; Rotter *et al.*, 2014; Fajuyitan *et al.*, 2015; 2017; 2018; Xu *et al.*, 2017) allowing the exploitation of two planes of symmetry for maximum computational efficiency (Fig. 3). A moment of magnitude equal to the reference elastic critical buckling

resistance M_{cl} (Eq. 2) was applied through a reference node which was linked kinematically to the displacement and rotational degrees of freedom at the edge of the cylinder. The loaded edge was maintained rigidly circular throughout the analysis but was allowed to rotate and displace in the meridional direction. Material properties for isotropic steel were assumed with a Young's modulus E of 200 GPa and a Poisson ratio ν of 0.3, although the outcomes are linear in E and may be extended to any isotropic elastic material.

$$M_{cl} = \frac{\pi}{\sqrt{3\left(1-\nu^2\right)}} Ert^2 \tag{2}$$

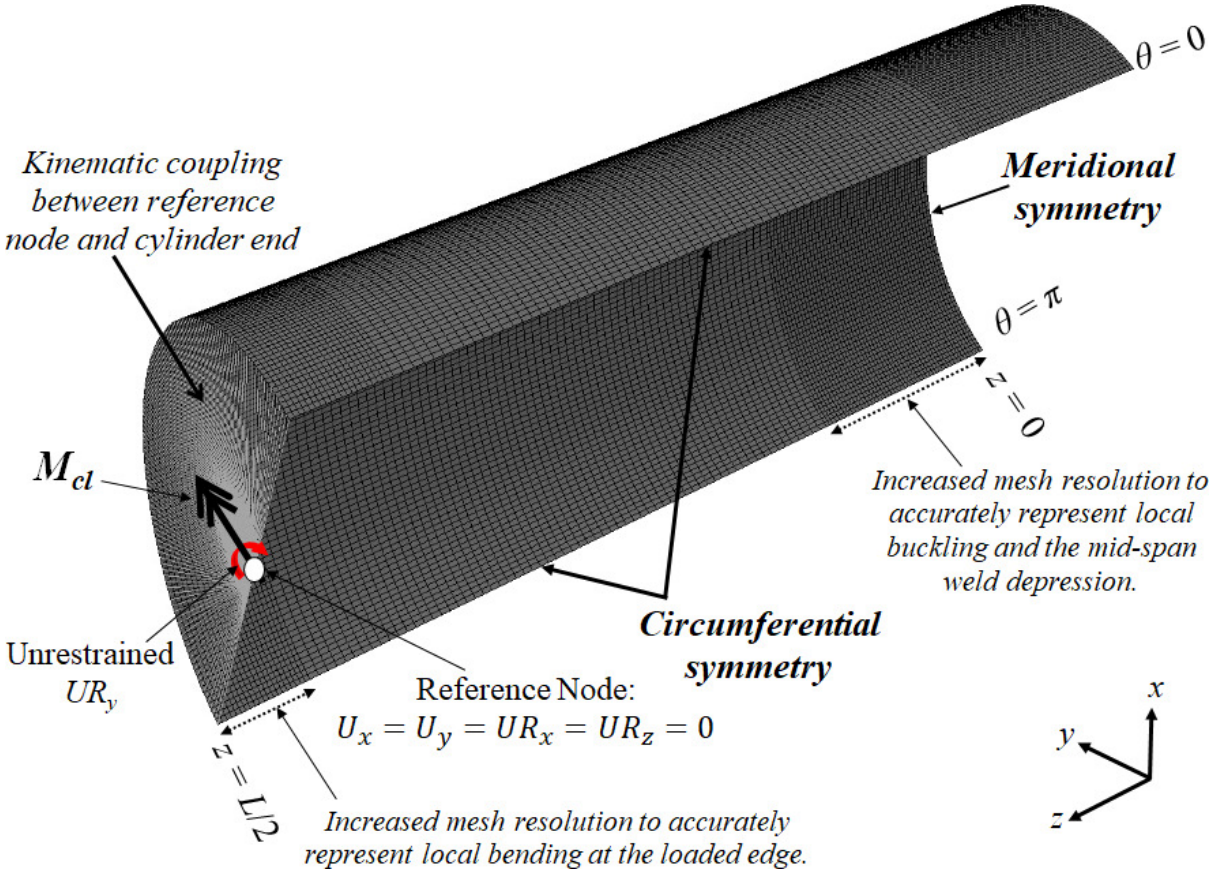

Fig. 3 – Generic details of the finite element quarter-shell model template.

Fajuyitan *et al.* (2015; 2018) showed that the degree of restraint of the rotations in the meridional direction about the circumferential loaded edge had a significant effect on the elastic buckling behaviour within the 'short' and 'medium' length domains (Fig. 1), with an unrestrained condition leading to lower buckling moments across a wide range of lengths. Consequently, the present study of imperfection sensitivity also investigated the influence of allowing the rotational degrees of freedom at the loaded edge to be either restrained or

unrestrained, respectively representing rotationally clamped (BCr) and simply-supported (BCf) boundary conditions.

The robust, general-purpose 4-node doubly curved shell element with reduced integration S4R was used in every model. The mesh resolution was refined significantly in the vicinity of the loaded edge to model the high local compatibility bending deformations correctly. Similarly, the mesh was also refined at the middle span where both eigenmode and weld depression imperfections were situated and local buckling was anticipated (Fig. 3). In both of these regions, the mesh was assigned a high meridional density of 20 elements per linear bending half-wavelength λ (Eq. 3) such that the element length was approximately $0.12\sqrt{(rt)}$.

$$\lambda = \frac{\pi\sqrt{rt}}{\left[3\left(1-\nu^2\right)\right]^{0.25}} \approx 2.444\sqrt{rt} \text{ for } \nu = 0.3 \tag{3}$$

Outside these zones of refinement, the cylindrical shell is expected to be predominantly under membrane action and a coarser mesh resolution was applied for efficiency.

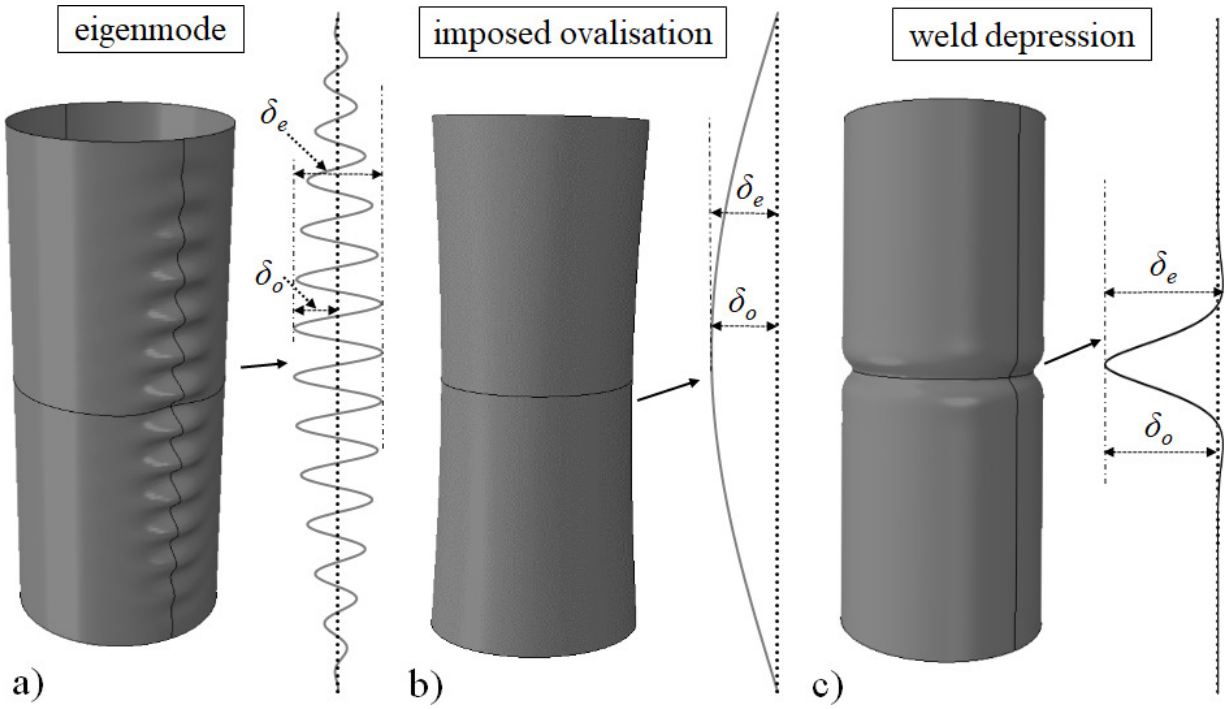

Fig. 4 – Illustration of the geometric imperfection forms employed and the 'equivalent geometric deviation' δ_e considered along the most compressed meridian.

3.2. Geometric imperfection forms

3.2.1. Critical linear bifurcation eigenmode imperfection

The widespread adoption of linear eigenmode imperfections defined by mathematically-convenient trigonometric functions originates from Koiter's (1945; 1963) perturbation analyses, the first studies to provide a reasonably accurate theory explaining the long-standing discrepancies between theoretical buckling stress predictions and experimental buckling loads of cylindrical shells under uniform axial compression (Bushnell, 1985; Rotter, 2004). It was long adopted thereafter that imperfections in the form of the critical linear eigenmode of the perfect shell, and axisymmetric eigenmodes in particular (circumferential harmonic zero), caused the greatest reduction in buckling strength in cylinders under uniform axial compression (Rotter, 2004), coincidentally also the most common and imperfection-sensitive shell system. Consequently, the eigenmode-affine pattern is prescribed as the 'default' imperfection form for the computational analysis of shells of any geometry and loading by EN 1993-1-6 (2007) where no other unfavourable form can be justified. For cylinders under uniform bending in the 'medium' domain or longer, the critical linear eigenmode computed by a linear bifurcation analysis (LBA) exhibits a series of closely-spaced local axial compression buckles on the compressed meridian (Fig. 4a; Rotter *et al.*, 2014) forming at a moment very close to the M_{cl} prediction (Eq. 2). ABAQUS conveniently permits this pre-computed geometry to be scaled to an appropriate amplitude δ_0 and imported as a mesh imperfection into a geometrically nonlinear analysis.

3.2.2. Imposed ovalisation imperfection

Cross-section ovalisation in long cylindrical elastic shells under bending is known to reduce the theoretical nonlinear buckling resistance of a cylinder by almost a half (Brazier, 1927; Tatting *et al.,* 1997; Karamanos, 2002; Li & Kettle, 2002). However, ovalisation was shown to be prevented if the dimensionless length of the cylinder falls below $\Omega = 0.5$ (Eq. 1b; Fig. 1; Calladine, 1983; Rotter *et al.,* 2014) because the rigid-circular boundary condition at the ends of the cylinder effectively restrains flattening of the cross-section at midspan. Given this phenomenon's potentially severe effect on the bending resistance, it is briefly explored here if the bending of an already slightly ovalised cylinder causes large buckling strength reductions to initiate at lengths shorter than $\Omega = 0.5$. The functional form defined in Eq. 4 (Sadowski & Rotter, 2013a) is used to generate the imperfect geometry explicitly. The single meridional half-wave ensures the cylinder remains circular at the edges ($z = 0$, L) but exhibits a

circumferential ovalising harmonic two at midspan ($z = L/2$) of maximum amplitude δ_0 (Fig. 4b) on the compressed meridian.

$$\delta = \delta_0 \cdot \sin\left(\frac{\pi z}{L}\right) \cdot \cos\left(2\theta\right) \tag{4}$$

3.2.3. Axisymmetric circumferential weld depression imperfection

Uniform bending induces a sinusoidally-varying meridional membrane stress state in the form of circumferential harmonic one, but the region of buckling-inducing membrane compression is wide and smooth enough to produce conditions approaching that of uniform compression. Consequently, it may be expected that an axisymmetric imperfection, so deleterious for uniform compression (Hutchinson & Koiter, 1970; Rotter, 2004), may be similarly deleterious for uniform bending. For this reason, the 'Type A' axisymmetric circumferential weld depression imperfection of Rotter and Teng (1989) was adopted (Eq. 5), a realistic representation of common manufacturing defects found in civil engineering shells (Berry *et al.,* 2000; Pircher *et al.,* 2001), with a single instance placed at midspan (Fig. 4c).

$$\delta = \delta_0 \cdot \exp\left(-\frac{\pi}{\lambda}\left|z-\frac{L}{2}\right|\right) \cdot \left\{\cos\left(\frac{\pi}{\lambda}\left|z-\frac{L}{2}\right|\right) + \sin\left(\frac{\pi}{\lambda}\left|z-\frac{L}{2}\right|\right)\right\} \tag{5}$$

3.2.4. Definition of an 'equivalent geometric deviation' δ_e

To allow for a commensurate comparison of buckling sensitivity to varying imperfections, the imperfection amplitudes δ_0 of all three imperfection forms were reformulated in terms of an 'equivalent geometric deviation' parameter δ_e (Eq. 6). This is defined here in terms of the maximum variation from 'peak to trough' of the imperfection form (Fig. 4), or the distance from the most inward to most outward radial position along the most compressed meridian. This adjustment accounts for the fact that, for example, though the amplitude of a sinusoidal wave is defined mathematically as δ_0 (Eq. 4), it is in fact only approximately half of the amplitude of the total geometrical deviation that the shell is subject to (for further details please see Rotter, 2004; 2016c).

$$\delta_e = \begin{cases} 2\delta_0 & \left(\text{eigenmode}\right) \\ \delta_0 & \left(\text{imposed ovalisation}\right) \\ 1.04\delta_0 & \left(\text{weld depression}\right) \end{cases} \tag{6}$$

3.3. Summary of parameter studies and automation of computational analyses

A linear elastic bifurcation analysis (LBA) is performed in ABAQUS as a matrix eigenvalue calculation employing a full 3D shell theory with both bending and membrane action. It is used to compute the critical linear bifurcation moment $M_{LBA} = M_{cr}$ of the perfect shell and to generate a file containing the scalable geometry of the eigenmode imperfection forms. A geometrically nonlinear analysis of the perfect (GNA) or imperfect (GNIA) shell may be performed as an equilibrium path-tracing analysis in ABAQUS with the modified Riks (1979) arc-length algorithm. It identifies the nonlinear characteristic buckling load M_{GNA} or $M_{GNIA} = M_k$ and the corresponding incremental buckling mode. The equilibrium path followed is the applied end moment M against the end rotation UR_y (Fig. 3). These predictions are used to construct the 'elastic reduction factor' RRD parameter α (Fig. 2), a product of a reduction due to geometric nonlinearity (α_G) and imperfection sensitivity (α_I):

$$\alpha\left(L,\delta_e\right)=\frac{M_{GNIA}\left(L,\delta_e\right)}{M_{LBA}\left(L\right)}=\frac{M_{GNIA}\left(L,\delta_e\right)}{M_{GNA}\left(L\right)}\cdot\frac{M_{GNA}\left(L\right)}{M_{LBA}\left(L\right)}\equiv\alpha_I\left(L,\delta_e\right)\cdot\alpha_G\left(L\right) \tag{7}$$

This study is divided into three parts. The first part presents buckling moment predictions for perfect and imperfect elastic cylinders of varying length (ω and Ω; Eq. 1), end rotational restraint conditions (BCr and BCf), imperfection form and imperfection amplitude. As the dimensionless lengths ω and Ω were found by Rotter *et al.* (2014) to permit the moment-length relationship (Fig. 1) for perfect cylinders to be represented independently of the r/t ratio, a single representative value of $r/t = 100$ was employed at this stage. For BCr, 32 lengths were investigated between $\omega = 5$ and 50 (i.e. $\omega = 50$ is $\Omega = 0.5$ for $r/t = 100$) within the 'medium' domain, with a higher resolution of lengths between $\omega = 5$ and 15 to explore the waviness of the relationship in this region (Fig. 1). For BCf, 37 lengths were investigated between $\omega = 4$ and 50, since the 'medium' length domain is known to initiate at shorter lengths for this condition (Fajuyitan *et al.*, 2015; 2017a,b). In the 'transitional' and 'long' domains governed by Ω, 16 lengths were analysed in the range $\Omega = 1$ to 10. For every combination of length, boundary condition and imperfection form, 8 normalised equivalent geometric deviations δ_e/t of 0.1, 0.25, 0.35, 0.5, 0.75, 1.0, 1.5 and 2.0 were investigated with GNIAs, although LBAs and GNAs were also performed on the perfect shell at each combination of length and boundary condition. The study purposefully omits δ_e/t amplitudes deeper than 2.0 for the imposed ovalisation imperfection form as such geometries are closer

to elliptical cylinders than circular ones and were the focus of a recent dedicated study by Xu *et al.* (2017). A summary of the individual computational analyses is presented in Table 1.

Table 1 – Balance of analyses for the first part of the study (r/t = 100).

Boundary condition	Lengths ω	Lengths Ω	Imperfection forms	Amplitudes δ_e	LBAs	GNAs	GNIAs
BCr	32	16	3	8	32+16	32+16	(32+16)×8×3
BCf	37	16	3	8	37+16	37+16	(37+16)×8×3
				Total:	101	101	2,424

In the second part, the extent to which the findings of the first part may considered to be independent of the r/t ratio are explored through an additional set of GNIAs performed at varying Ω (i.e. only in the 'transitional' length domain), δ_e/t and r/t, as summarised in Table 2. In the third part, a non-increasing lower-bound length-dependent synthetic imperfection sensitivity relationship is constructed from the predictions for the three imperfection forms, and the authors offer an algebraic characterisation for the RRD α_I parameter.

Table 2 – Balance of analyses for the second part of the study (BCr only).

Constant	Lengths Ω	Ratios r/t	Imperfection forms	Amplitudes δ_e	GNIAs
δ_e/t	14	34	2	8	14×34×2×8
				Total:	7,616

The total number of individual analyses summarised in Tables 1 and 2 above is 10,242, an overwhelming number for an analyst to process individually if model generation, submission, termination and processing were to be performed manually. This study employs the analysis management strategy of Sadowski *et al.* (2017) which exploits the Python and FORTRAN programming languages interfacing with ABAQUS to automate each of the above operations. Key to the strategy is enforcing a set of 'kill conditions', any one of which automatically terminates an ongoing GNA or GNIA when triggered, the most important ones being:

- Terminate analysis when the current increment's load proportionality factor is less than that of the previous increment. This kill condition detects bifurcation or limit point buckling with unstable post-buckling equilibrium paths.

- Terminate analysis when the absolute relative difference between the current and previous incremental radii of curvature of the equilibrium curve exceeds a tolerance.

The latter kill condition was found to be particularly valuable where a deeper imperfection amplitude turns a bifurcation on the equilibrium path into a 'kink' with a smooth transition from pre- to post-buckling, accompanied by a visible growth in buckling deformations but with the solver reporting no loss of positive-definiteness in the global tangent stiffness matrix. This phenomenon of stable post-buckling behaviour at deeper imperfection amplitudes has been reported in cylindrical shells under various load cases (e.g. Yamaki, 1984; Rotter, 2007; Sadowski & Rotter, 2011a; Sadowski *et al.*, 2017) and naturally leaves an analyst in doubt of which criterion to use in establishing a conservative buckling load.

4. Individual predicted moment-curvature relationships

The elastic buckling behaviour of perfect cylinders in the 'medium', 'transitional' and 'long' length domains is introduced here with the aid of predicted moment-curvature equilibrium curves (Fig. 5). The mean curvature φ over the full length of the cylinder was obtained from the computed rotation UR_y of the rigid circular cross-section at the ends (Eq. 8a; Fig. 3). It was subsequently normalised by the buckling curvature φ_{cl} (Eq. 8b) from beam theory:

$$\varphi = \frac{2 \cdot UR_y}{L} \text{ and } \varphi_{cl} = \frac{t}{r^2\sqrt{3\left(1-\nu^2\right)}} \approx 0.605\frac{t}{r^2} \text{ for } \nu = 0.3 \qquad (8a,b)$$

In the 'medium' length domain, the effect of employing a weaker rotational restraint at the edges is manifest as a minor reduction in the buckling moment from ~0.92M_{cl} to ~0.90M_{cl} for the BCr and BCf conditions respectively (Figs 1 and 5). The slightly lower predictions for the BCf condition are due to the buckle forming near the loaded edge rather than at midspan as for the BCr condition (Fig. 6), a simultaneous consequence of a locally-perturbed membrane stress state and a lack of rotational restraint within the bending boundary layer at the cylinder edges. It should be recognised that realistic practical boundary conditions lie somewhere between the limiting cases of BCr and BCf, both of which anyway predict very similar behaviour for perfect cylinders in the 'medium' length domain (Fig. 5a), and that a finite rotational stiffness restraint would thus not lead to significantly different behaviour. Similarly, for the predictions of imperfect cylinders that follow, these two boundary conditions should equally be seen as limiting cases with the 'real' condition falling

somewhere in-between. Within the 'transitional' domain, the influence of varying rotational restraint condition at the edges has no further influence at all on either the equilibrium path, the critical buckling moment or the buckling location (Fig. 5b). Instead, as pre-buckling ovalisation becomes progressively more severe with length, the moment-curvature relationship becomes increasingly nonlinear and buckling occurs at midspan at lower moments (Fig. 5c), with ovalisation becoming fully-developed within the 'long' domain.

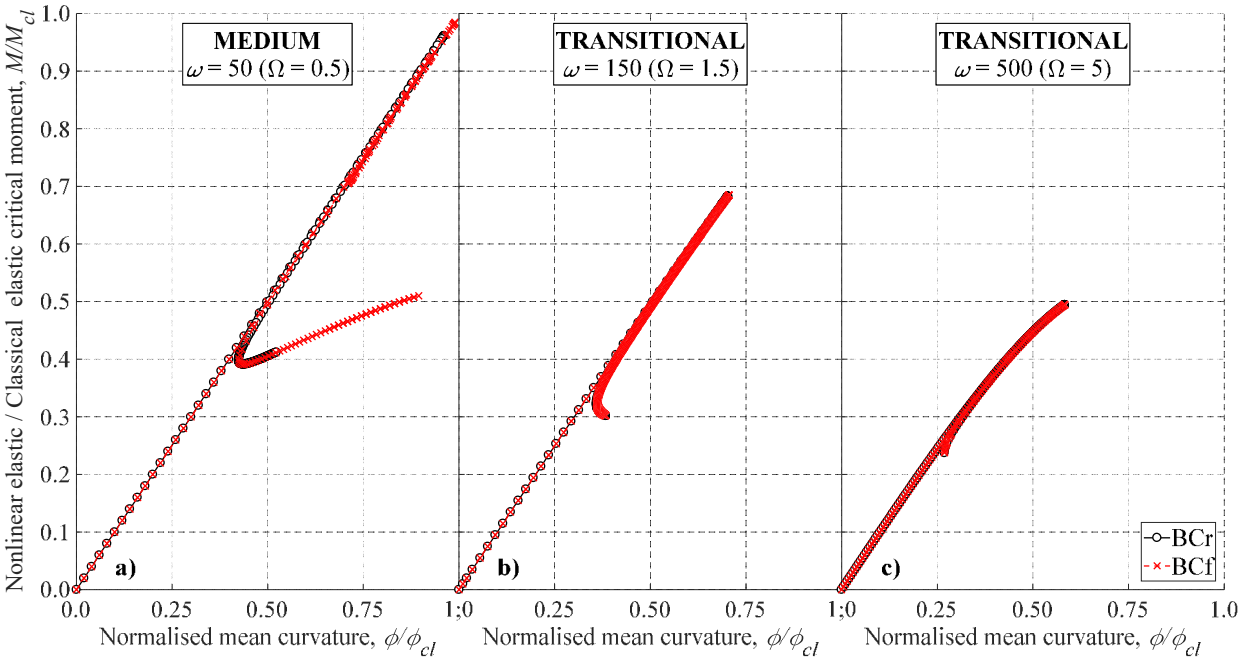

Fig. 5 – Predicted moment-curvature relationships for perfect cylinders under bending in three length domains and under two sets of end restraint conditions (r/t = 100).

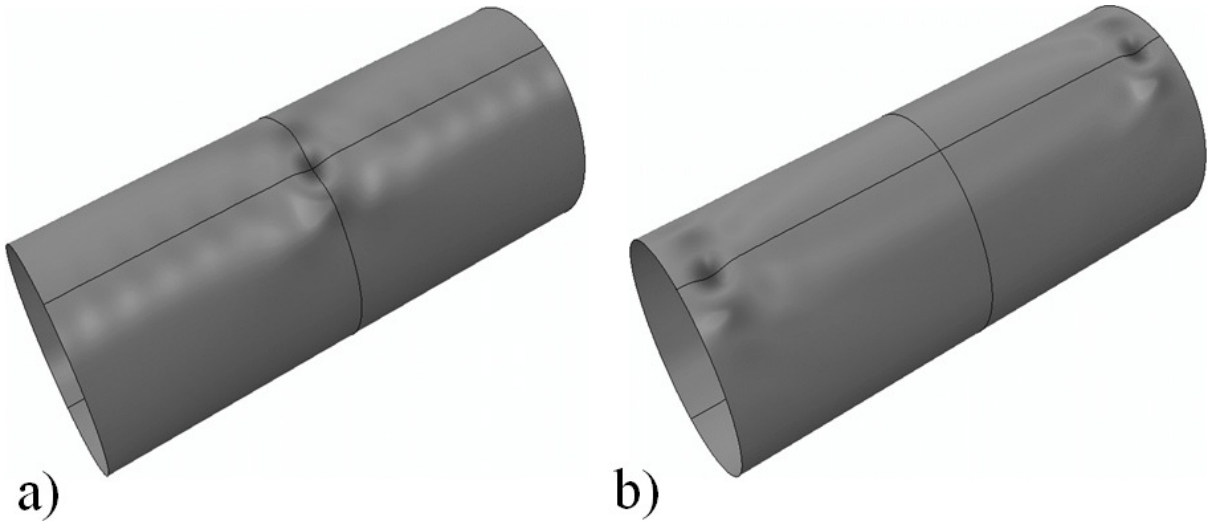

Fig. 6 – Incremental buckling modes for cylinders of 'medium' length (ω = 50) showing the different location of buckles under a) BCr and b) BCf end support conditions.

The predicted elastic buckling resistance of cylinders of 'medium' length appears to be very dependent on the form and amplitude of the applied initial geometric imperfections (Fig. 7). For example, at very small amplitudes ($\delta_e/t < 0.50$), BCr cylinders are most susceptible to eigenmode imperfections, while the imposed ovalisation imperfection has a neutral effect on the predicted buckling strength. However, at deeper imperfections ($\delta_e/t \geq 0.5$), the weld depression becomes the most deleterious and reduces the buckling strength by up to 65% at $\delta_e/t = 1.5$, while the imposed ovalisation imperfection becomes either only mildly detrimental or remains neutral. In addition, from $\delta_e/t \geq 1.0$, the equilibrium path of the cylinder under the weld depression gradually changes from one exhibiting obvious bifurcation buckling with a steeply-descending post-buckling path (red curve in Fig. 7) to one exhibiting only a 'kink' with a smooth transition from pre- to post-buckling and a corresponding growth in buckling deformations, with no negative eigenvalues detected in the global tangent stiffness matrix by the solver at any point. In such cases the buckling moment was conservatively taken as that corresponding to the 'kink' as advised by EN 1993-1-6 (2007), automatable using the second of the aforementioned 'kill conditions'.

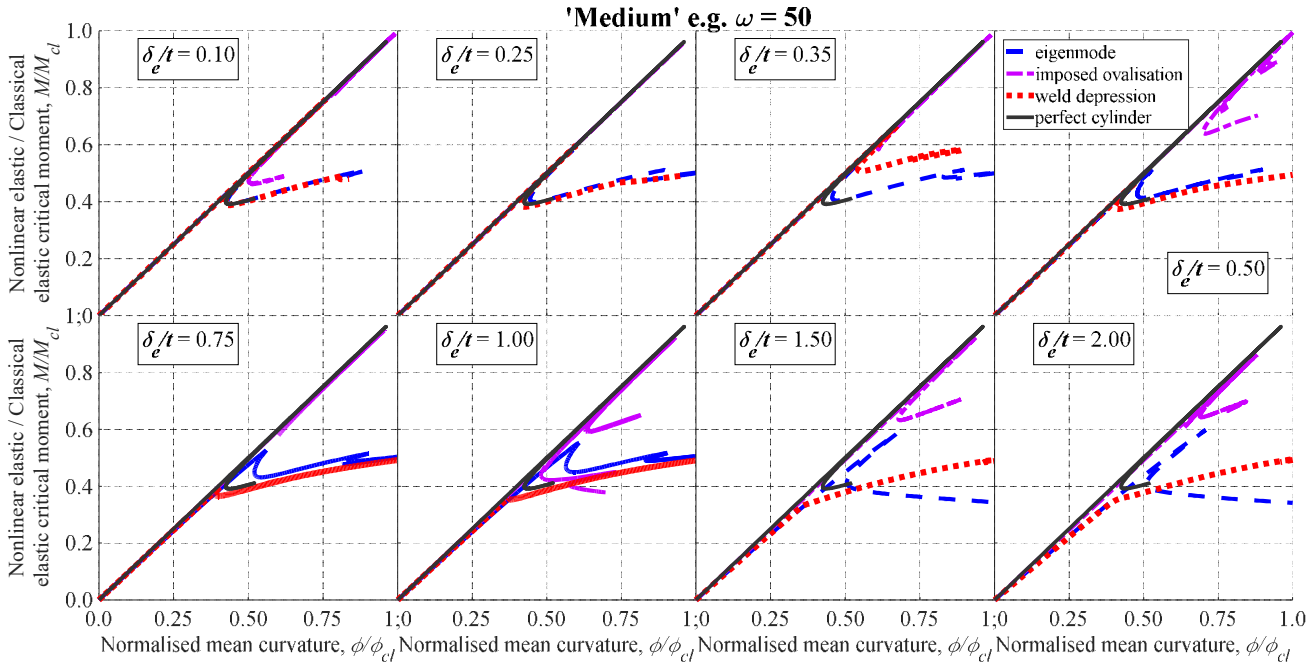

Fig. 7 – Normalised moment-curvature relationships for increasingly imperfect cylinders of 'medium' length ($\omega = 50$ or $\Omega = 0.5$) with the BCr end support condition.

In the 'transitional' length domain, there is a complex interaction between local buckling, cross-sectional ovalisation and imperfections potentially resulting in a combined loss of up to

75% of the theoretical buckling strength M_{cl} of the cylinder (Fig. 8). While this imperfect behaviour is again greatly dependent on both the form and amplitude of the imperfections, the weld depression imperfection consistently controls as the most deleterious imperfection. The imposed ovalisation imperfection has an almost entirely neutral effect in this length domain, suggesting that initially slightly ovalised cylinders are not especially vulnerable to reductions in buckling load arising from further ovalisation under bending than initially perfect cylinders.

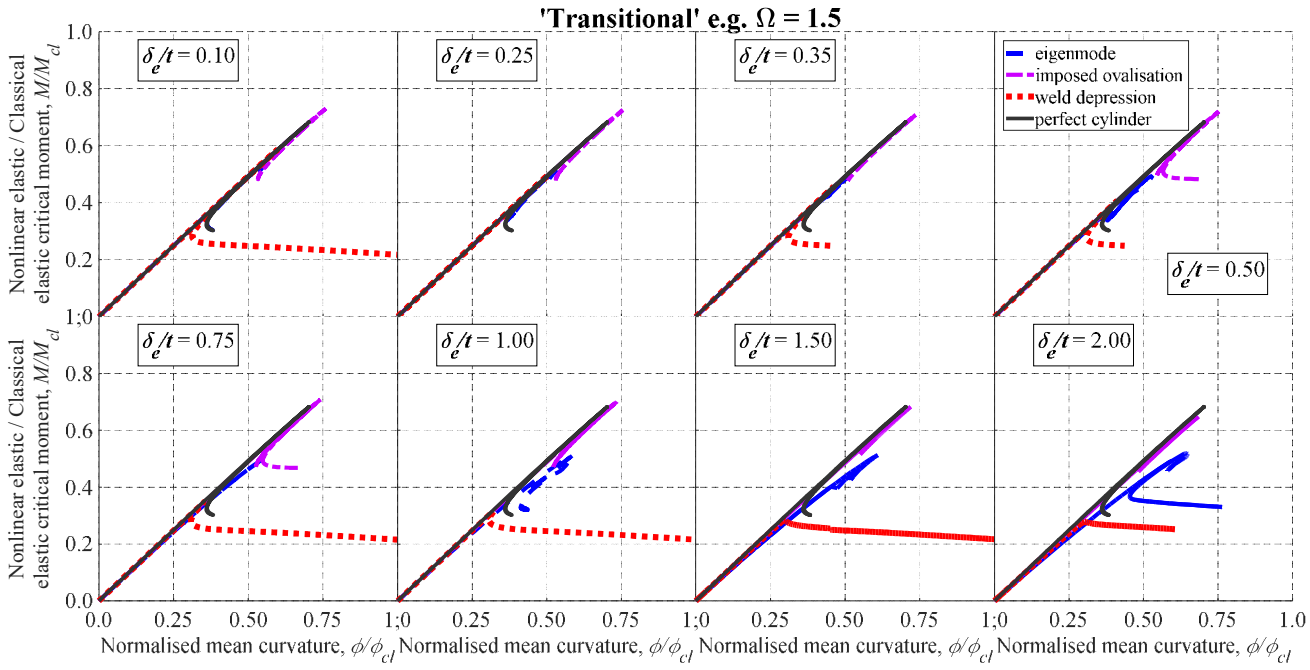

Fig. 8 – Normalised moment-curvature relationships for imperfect cylinders of 'transitional' length (ω = 150 or Ω = 1.5) with the BCr end support condition.

5. Influence of cylinder length on imperfection sensitivity

Classical imperfection sensitivity relationships for selected lengths across three length domains and for the three different imperfection forms are illustrated in Fig. 9 as plots of the ratio of the buckling strength of the imperfect cylinder to that of the perfect cylinder $\alpha_I = M_{GNIA} / M_{GNA}$ (Eq. 7) against the equivalent geometric deviation δ_e/t. These results suggest that the longest cylinders still in the 'medium' length domain (i.e. as $\omega \rightarrow 50$ or $\Omega \rightarrow 0.5$) demonstrate the most severe sensitivity to the two most serious considered imperfection forms. At the 'medium' to 'transitional' domain boundary, the pre-buckling behaviour is dominated by smooth membrane action with little geometric nonlinearity, characteristic of

other well-known systems with severe imperfection sensitivity such as cylindrical shells under uniform compression or spherical shells under uniform external pressure (Thompson & Hunt, 1973; 1984). Cylinders shorter than $\omega = 50$ but still in the 'medium' domain become increasingly constrained by the edge boundary condition where compatibility bending has a greater contribution to the pre-buckling stress state, manifest as a gradual mollifying of imperfection sensitivity as $\omega \rightarrow 0$. None of these computed relationships suggest as severe an imperfection sensitivity as for cylinders under uniform compression, as illustrated through the comparison in Fig. 9 with well-known relationships from Koiter (1945) and Rotter & Teng (1989). Also shown is a comparison with the computational study by Chen *et al*. (2008) who established the first tentative relationship for α_I for cylinders under uniform bending with the same weld depression imperfections. Quite fortuitously, the α_I expression proposed by these authors appears to correspond to the worst possible imperfection sensitivity for this system, despite being established on the basis of a single dimensionless length of $L/r = 7$.

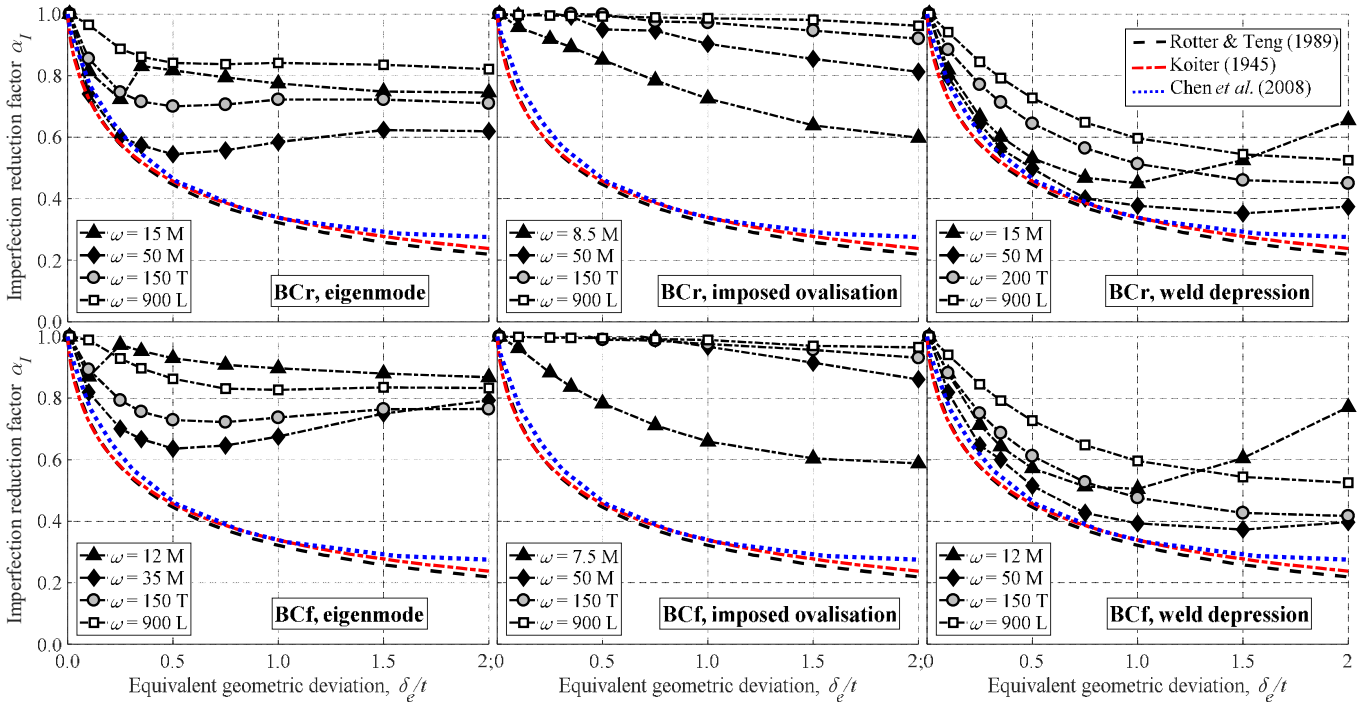

Fig. 9 – Computed imperfection sensitivity relationships of α_I vs δ_e/t for elastic cylinders under bending in the three length domains and for three imperfection forms (here 'M', 'T' and 'L' identify lengths in the 'medium', 'transitional' and 'long' domains respectively).

The imposed ovalisation imperfection was found to have a consistently neutral effect, with a predicted reduction in buckling moment of only ~10% for $\delta_e/t = 2$ at the 'most severe' length

of ω = 50, with the sensitivity to this imperfection almost vanishing for longer ovalising cylinders. An apparent exception may be seen for cylinders on the short side of the 'medium' length domain ($\omega \approx 8$), where this imperfection is seen to cause up to an ~40% reduction in the buckling moment for $\delta_e/t = 2$. However, while the predictions for such short cylinders are presented here for completeness, it should be stressed that such cylinders are unlikely to be subject to such artificially-imposed ovalisation imperfections in practice as the end boundary conditions, which maintain circularity of the cross-section, would be very effective in restraining such deformations. Consequently, these predictions are not considered further here.

The complete computed relationships between the normalised buckling moment M_k / M_{cr} and the dimensionless cylinder length ω (log scale) are presented in Figs 10, 11 and 12 for the eigenmode, imposed ovalisation and weld depression imperfections respectively for both BCr and BCf sets of boundary conditions. Data at constant ω used to form the individual imperfection sensitivity relationships shown in Fig. 9 are identified by a dotted oval. A closer inspection of the moment-length relationships for the eigenmode and weld depression imperfections (Figs 10 & 12) confirms that the imperfection sensitivity becomes increasingly severe with increasing length within 'medium' length domain, reaching a maximally detrimental effect at the boundary of the 'medium' to 'transitional domains ($\omega \approx 50$ or $\Omega \approx 0.5$), and then becoming milder with increasing length within the 'transitional' length domain as pre-buckling ovalisation becomes more important. All three imperfection forms tend to an 'asymptotic' and relatively mild imperfection sensitivity relationship within the 'long' length domain which is invariant with further changes in length. Here, ovalisation is fully-developed and is the main mechanism responsible for the significant reduction in the stiffness of the cylinder's fundamental response. Although the buckling response does not strictly pass a limit point due to local buckling always occurring on the flattened side at a critical moment approximately 5% below the predicted limit point moment (Karamanos, 2002; Xu *et al.*, 2017), the system essentially behaves like a limit point one with imposed imperfections having only a modestly deleterious influence. Similar behaviour is documented in other systems with a highly nonlinear fundamental path that similarly exhibit a milder imperfection sensitivity than those with a linear fundamental path (Thompson & Hunt, 1973; 1984).

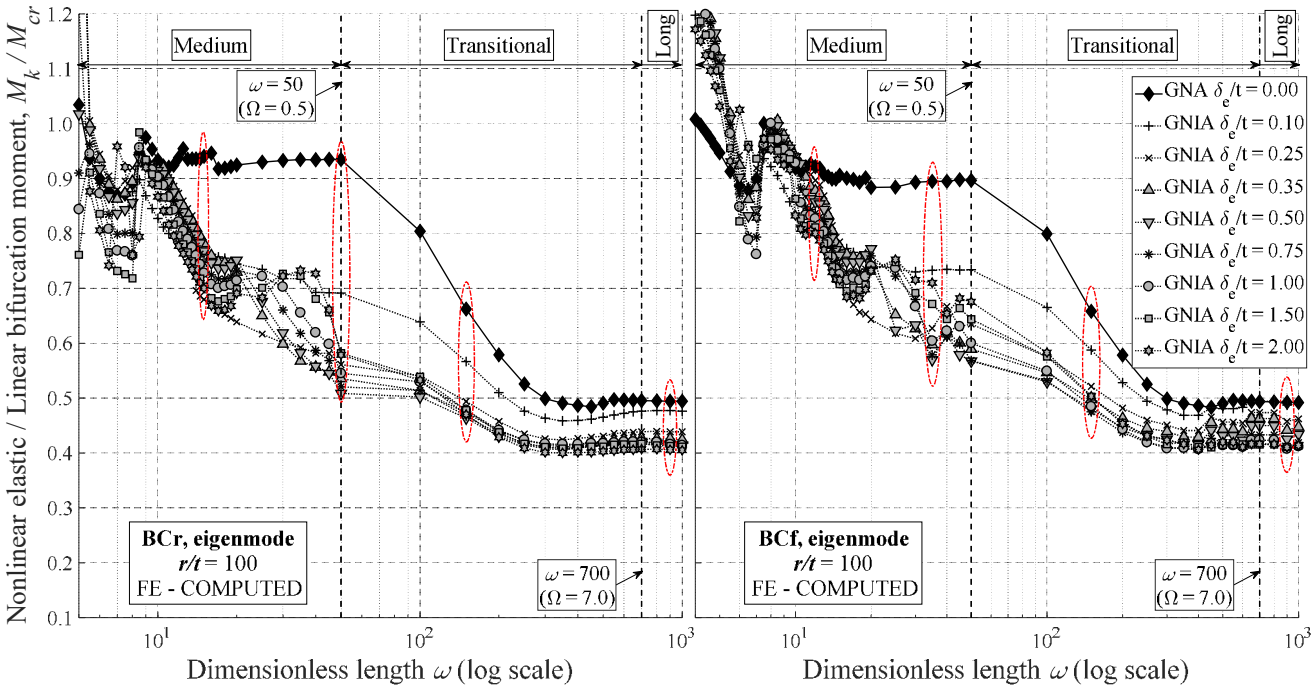

Fig. 10 – Computed relationships between M_k / M_{cr} and ω for elastic cylinders under uniform bending and the critical linear buckling eigenmode imperfection form.

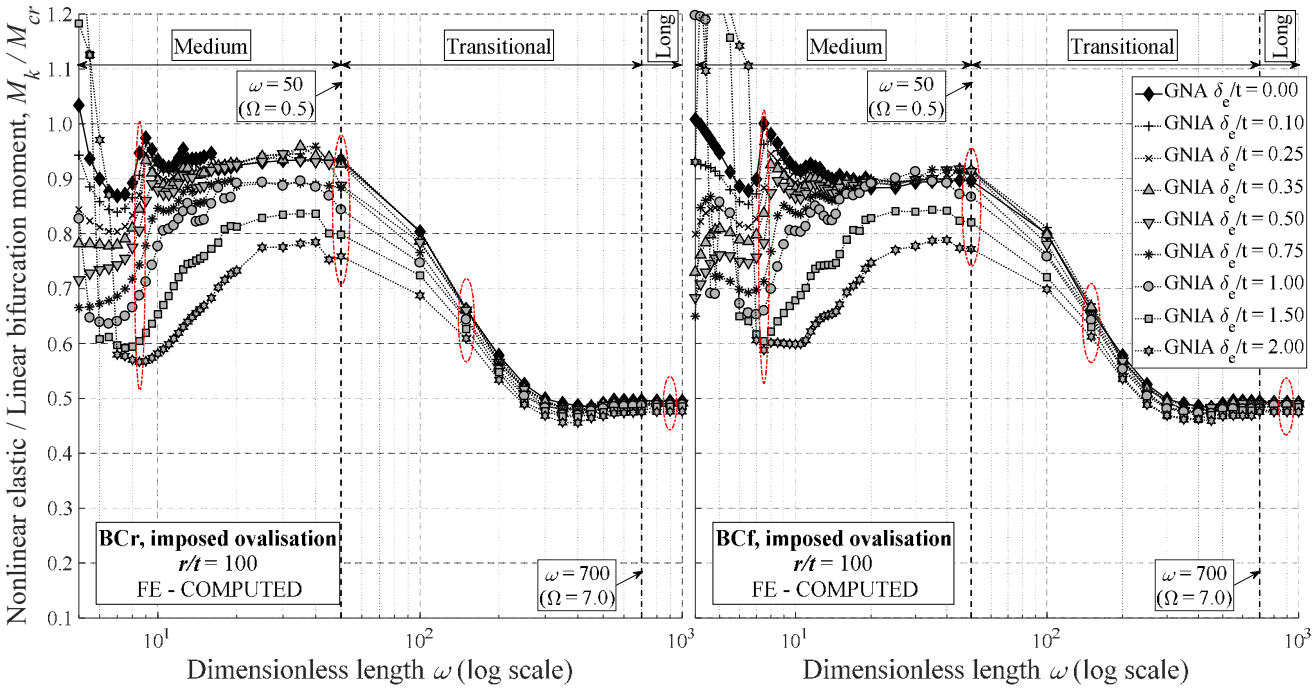

Fig. 11 – Computed relationships between M_k / M_{cr} and ω for elastic cylinders under uniform bending and the imposed ovalisation imperfection form.

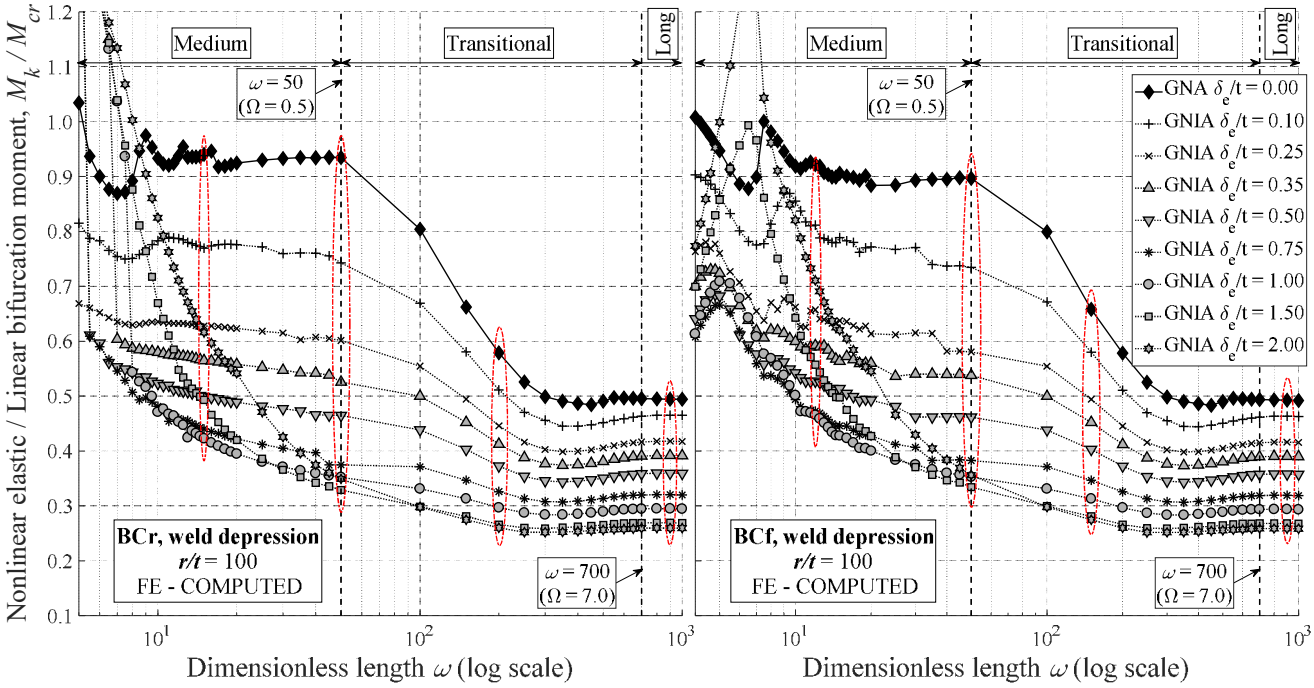

Fig. 12 – Computed relationships between M_k / M_{cr} and ω for elastic cylinders under uniform bending and the axisymmetric circumferential weld depression imperfection form.

The relationship between the moment and length is significantly smoother and better defined for the weld depression than for the eigenmode imperfection. This is because the geometry of the weld depression follows a strict mathematical definition that is invariant with length (Eq. 5), whereas the shape of the eigenmode imperfection is computed anew for each length from an LBA and the imperfection is thus slightly different every time. More importantly, the weld depression appears to almost always be the most severe imperfection form across all lengths, amplitudes and boundary conditions. This may be attributed to the fact that the region of pre-buckling membrane compression is both smooth and wide enough circumferentially to approach conditions that are approximately uniform, and under uniform compression it is well documented that axisymmetric imperfection forms are the most damaging (Hutchinson & Koiter, 1970; Rotter, 2004). The shape of the eigenmode is always localised in nature with a high circumferential wave number (Fig. 4), thus it cannot be as detrimental in a region of smooth and near-uniform membrane compression as the weld depression, which is axisymmetric by design.

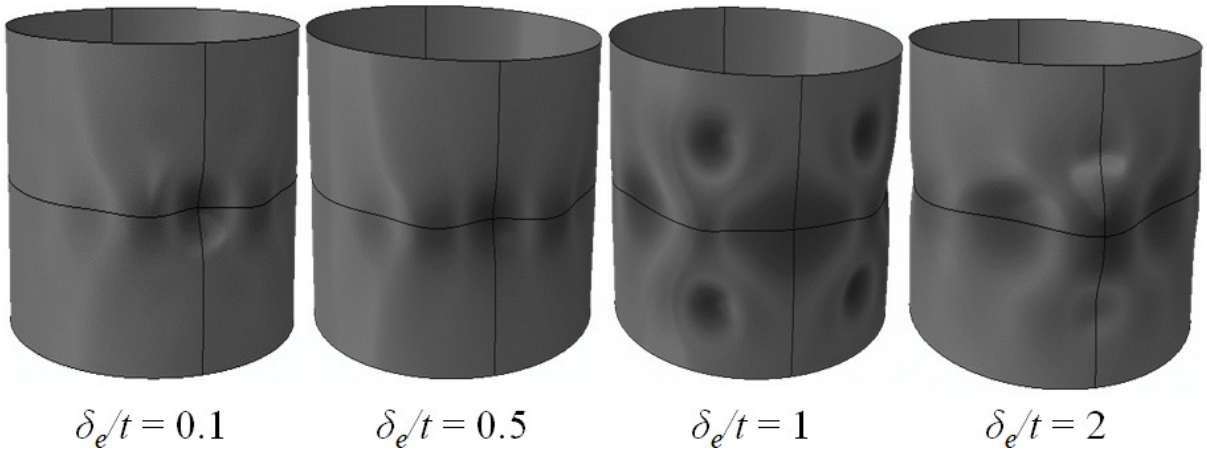

Fig. 13 – Selected incremental buckling modes of quite short cylinders still in the 'medium' length domain (ω = 15) with the weld depression imperfection form showing the growing size of the buckle with imperfection amplitude δ_e/t to the extent that it interferes with and is constrained by the end boundary conditions.

For increasingly shorter cylinders, the eigenmode and, in particular, the weld depression imperfections may exhibit a non-decreasing relationship with increasing imperfection amplitude δ_e/t where, in effect, a deeper imperfection causes a rise in buckling strength. This stiffening effect may be substantial, causing rises in buckling strength to well above that of the perfect cylinder, such that $\alpha_I > 1$. This is because a deeper imperfection causes the buckling mode to involve more of the length of the shell (see Fig. 8 in Rotter & Teng, 1989), and for these rather short cylinders the buckling mode eventually begins to encroach upon and become constrained by the edge boundary conditions, as illustrated in Fig. 13. The phenomenon of deeper imperfections causing a rise in buckling strength has been documented before in computational studies of imperfection sensitivity in cylindrical shells under unsymmetrical loading conditions (e.g. Sadowski & Rotter 2012; 2013b) and poses a problem in establishing codified imperfection sensitivity relationships for use in design. The Eurocode on Metal Shells EN 1993-1-6 (2007) provides a safeguard against this eventuality for designers using the 'GMNIA' procedure to design a shell by requiring the analysis to investigate an imperfection amplitude 10% smaller than the codified value. Where this second analysis is found to predict a lower buckling strength, the analyst is obliged to adopt an iterative procedure and effectively reproduce full imperfection sensitivity relationship to establish the minimum. A strategy that does not burden the analyst with this onerous procedure whilst leading to a conservative codified relationship for α_I for use in RRD is presented at the end of this paper.

6. Influence of cylinder *r/t* ratio on imperfection sensitivity

The preceding section presented detailed relationships between the predicted buckling moment and the cylinder length at a single *r/t* ratio of 100, on the hypothesis that formulating these results in terms of the dimensionless length variables ω (and Ω) allows the behaviour to be expressed independently of the *r/t* ratio. By way of verification, an additional set of GNIAs for varying *r/t* from 100 to 500 were performed within the 'transitional' length domain for Ω from 0.5 to 7, as summarised in Table 2. It was sufficient to restrict this analysis to this length domain only because the behaviour here was independent of the boundary condition and because its shortest portion (i.e. at $\Omega = 0.5$) contained the length region with the 'most severe' imperfection sensitivity as identified previously. A selection of the critical buckling moment predictions is presented in Fig. 14 in the form of 'modified' capacity curves of M_k / M_{pl} vs M_k / M_{cr}, a construct designed to allow a convenient extraction of the RRD algebraic parameters, though in the absence of plasticity only $\alpha = \alpha_G \times \alpha_I$. Assuming that the correct dimensionless group governing the geometrically nonlinear buckling behaviour has been identified (i.e. Ω), computed capacity curves *should* appear as vertical lines in this space (Fig. 2b) indicating an invariant relationship between M_k / M_{cr} and the cylinder slenderness (obtained by varying the *r/t* ratio) and allowing the corresponding α value to be simply read off the horizontal axis. Thicker cylinders with *r/t* near 100 have the highest M_k / M_{pl} resistances and are thus in the upper regions of each curve, while thinner cylinder with *r/t* approaching 500 have the lower M_k / M_{pl} resistances and thus may be found lower down. It should be added that the yield strength of the material is not relevant to this discussion as changing it would only alter the scaling of the vertical axis. For the purposes of constructing Fig. 14, a generic grade with a 460MPa yield stress was assumed. Only the eigenmode and weld depression imperfections were considered in this analysis.

The elastic 'modified' capacity curves shown in Fig. 14 illustrate that the dimensionless group Ω, arising naturally in the analysis of *perfect* cylinders under unsymmetrical loading with small circumferential wave numbers, mostly maintains invariant geometric nonlinearity for ovalising cylinders under bending with eigenmode imperfections and leads to curves that are reasonably vertical. For the more severe weld depression imperfection, by contrast, grouping the data in terms of Ω no longer maintains verticality, especially for increasingly long and imperfect ovalising cylinders (i.e. simultaneously higher δ_e/t and Ω). In particular, capacity curves in the lower right-hand part of Fig. 14 exhibit an increase in M_k / M_{cr} with

increasing r/t beyond $r/t \approx 300$, suggesting that the weld depression acts as a stiffening corrugation against the circumferential bending induced by ovalisation (a similar effect was previously documented in Sadowski & Rotter, 2011b). An RRD characterisation based on predictions for the weld depression imperfection form performed at $r/t = 100$ will, with limited exceptions, constitute a conservative lower bound to the possible behaviour, and will form the data set used in the last part of this paper. Additionally, while it may be possible in future work to report a dimensionless group dependent on all of L, r/t and δ_e/t that would maintain invariance of M_k / M_{cr} with slenderness for long, imperfect, ovalising cylinders, such a group was not identified despite significant efforts and the choice was made to retain the Ω parameter for simplicity and consistency with the reference perfect system.

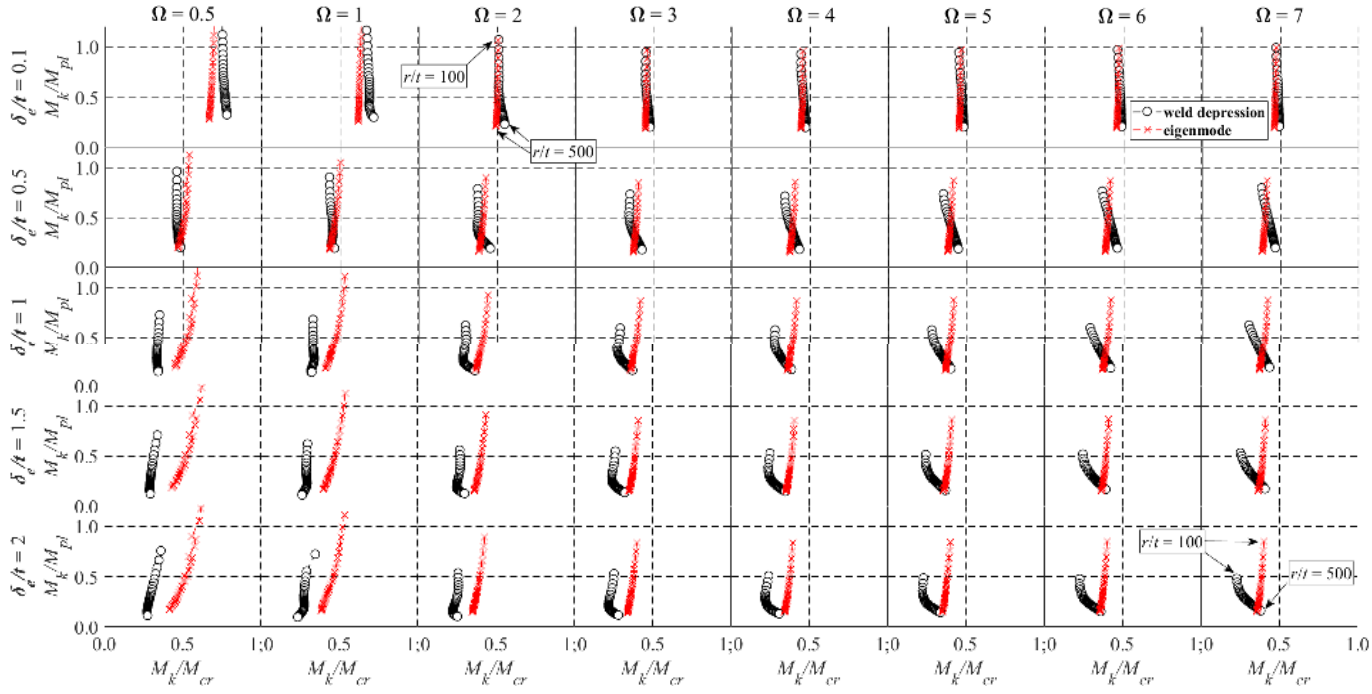

Fig. 14 – Elastic 'modified capacity curves' for cylinders under uniform bending with the eigenmode and weld depression imperfections in the 'transitional' length domain.

7. Algebraic characterisation of imperfection sensitivity for RRD

7.1. Introduction

The previous sections employed a validated computational tool to provide numerical evidence to establish detailed relationships for the sensitivity of cylindrical shells under uniform bending to three different imperfection forms. It was shown that the strength of the imperfect shell is strongly dependent on both the form and amplitude of the imperfection, as

well as on the cylinder length, the end boundary conditions and, to a lesser extent, the *r*/*t* ratio. This section undertakes a reduction of this data into a single lower-bound relationship more amenable to characterisation into conservative algebraic expressions for use in manual dimensioning within the RRD framework. The processing and characterisation of the generated result data was conducted using the MATLAB (2014) programming environment.

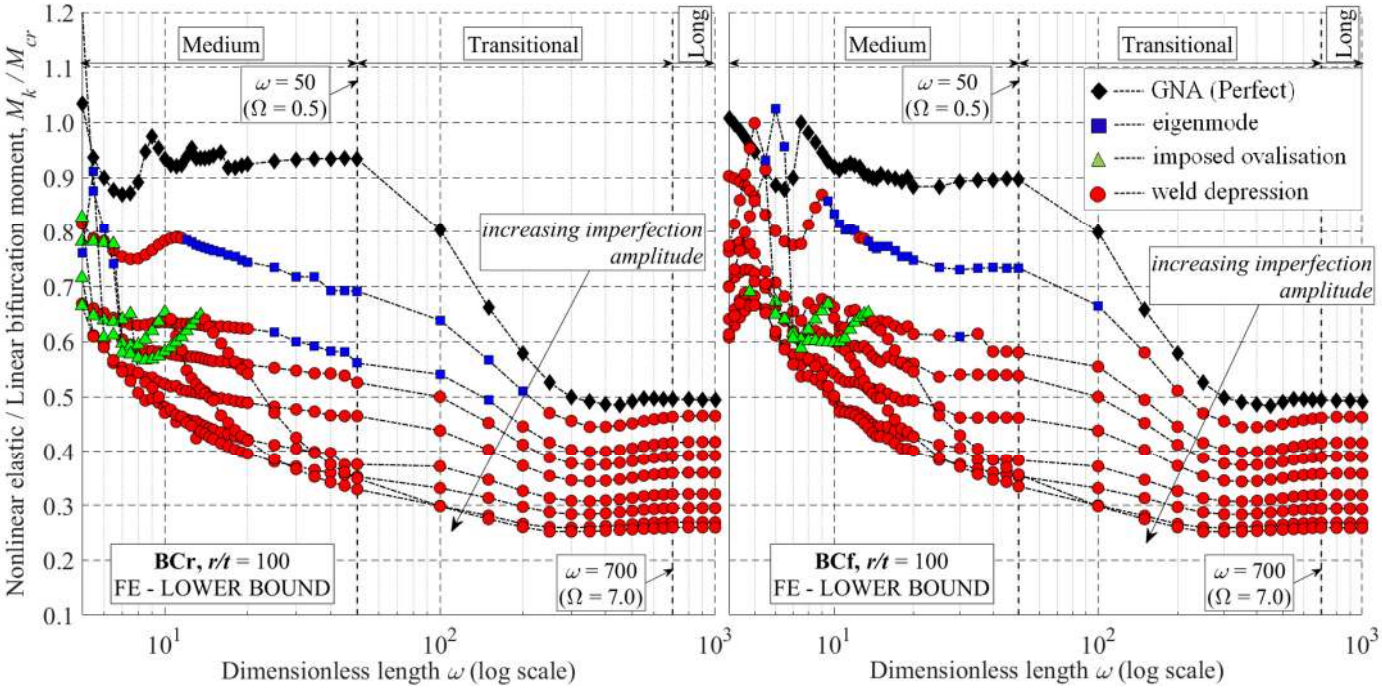

Fig. 15 – Lower-bound M_k / M_{cr} *vs.* ω relationships for BCr and BCf imperfect elastic cylindrical shells under uniform bending.

7.2. Construction of a synthetic length-dependent imperfection sensitivity relationship

The M_k / M_{cr} vs ω relationships at $r/t = 100$ for each of the three imperfection forms were first harmonised into a single set of relationships per boundary condition by identifying the minimum buckling strength out of the three imperfection forms at every combination of length ω and equivalent geometric deviation δ_e/t. This procedure loosely reflects the conservative lower-bound approach used in establishing the imperfection sensitivity relationship for axially-compressed cylindrical shells (Rotter, 2004), where the minimum buckling strengths were identified from a large database of test results. In addition to ensuring that the most detrimental prediction at each length is used as the basis for a conservative characterisation of the buckling behaviour of cylindrical shells under uniform bending, this procedure allows a definitive identification of which imperfection form is likely

to be most critical and where. The resulting lower-bound M_k / M_{cr} vs ω relationship is shown in Fig. 15 where it is suggested that, for modest to deep imperfections and across all length domains, the axisymmetric weld depression consistently controls as the most deleterious geometric imperfection. This figure is colour-coded to enable quick identification of the origin imperfection form for each data point.

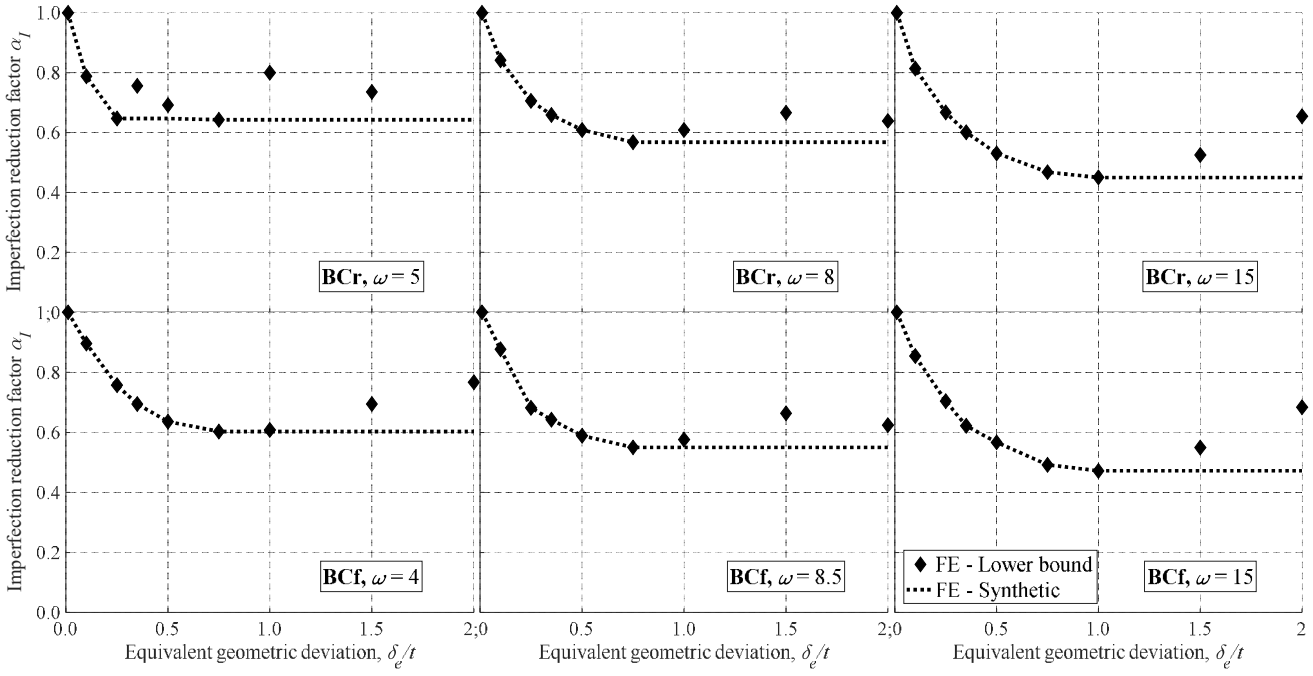

Fig. 16 – Synthetic imperfection sensitivity relationships of M_k / M_{cr} vs δ_e/t for BCr and BCf 'medium' length cylinders under uniform bending with r/t = 100.

It was shown previously that the weld depression imperfection may exhibit an increase in buckling strength for deeper imperfections in the 'medium' domain (Figs 9 & 12), a consequence of a buckling mode that grows with imperfection amplitude while encroaching upon and becoming constrained by the boundary condition (Fig. 13). This poses a challenge for any algebraic characterisation of imperfection sensitivity, as a conservative design rule should not lead the analyst to design a more imperfect shell for a higher resistance than a less imperfect one. At any length ω, a synthetic imperfection sensitivity relationship of M_k / M_{cr} vs δ_e/t was established where a buckling resistance at a larger value of δ_e/t was constrained to never exceed that at the preceding value of δ_e/t, as shown in Fig. 16. This correction was only necessary within the 'medium' length domain controlled by ω, but not in the 'transitional' or 'long' domains controlled by Ω as these domains are free of boundary effects. The resulting 'synthetic' lower-bound non-increasing moment-length relationships are illustrated in Fig. 17

for both end boundary conditions. As a fortuitous side-effect, the resulting curves are now more amenable for algebraic characterisation, especially in the 'medium' length domain where boundary effects previously led to rather messy moment-length relationships (compare the low ω ranges in Fig. 17 with those in Fig. 15).

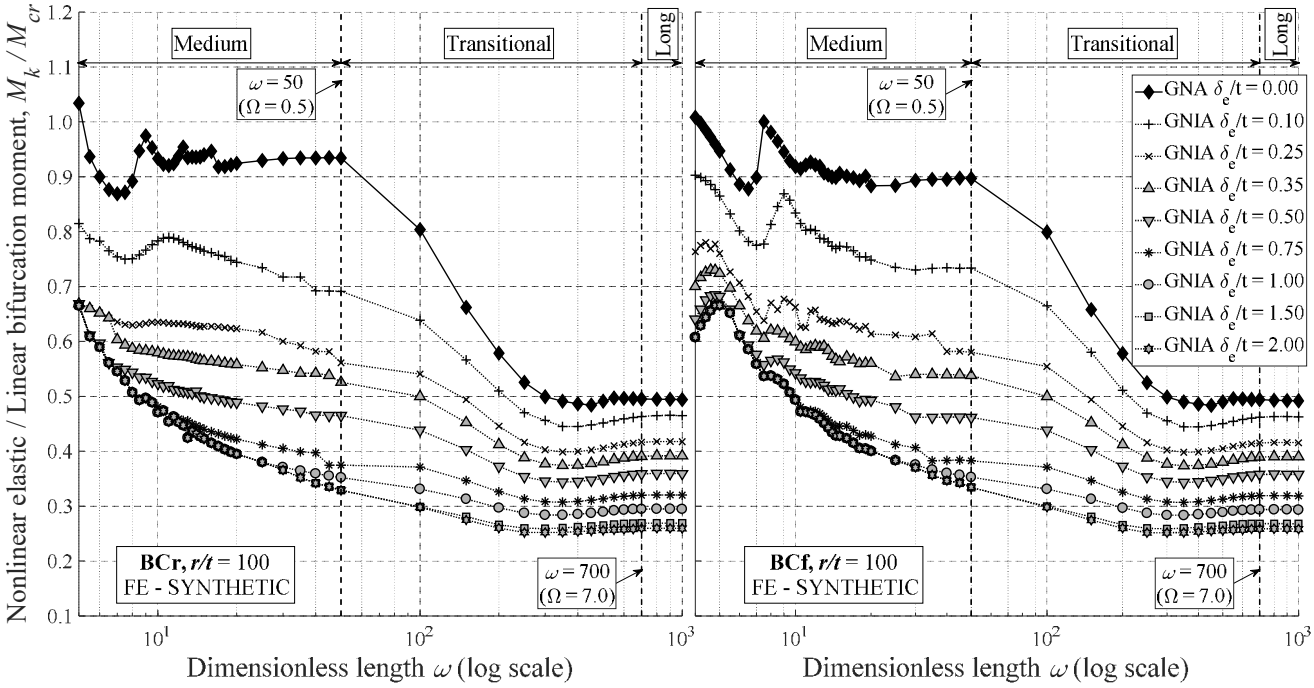

Fig. 17 – Synthetic M_k / M_{cr} *vs.* ω relationships for BCr and BCf imperfect elastic cylindrical shells under uniform bending.

7.3. Proposal for the elastic imperfection reduction factor α_I

The ultimate aim of this study is to characterise the buckling behaviour of imperfect cylindrical shells under uniform bending into algebraic expressions which can be used for conservative yet meaningful prediction of the buckling resistance. It is envisaged that the authors' proposal for α_I will be used within the RRD framework together with the geometrical reduction factor α_G already established Rotter *et al.*, (2014) and plasticity-related parameters λ_0, η_0, η_p and χ_h currently being established by Wang *et al.* (2018) to spare the designer from having to undertake a computational analysis to determine the fully nonlinear resistance of a cylindrical shell under uniform bending. It is hoped that more systems will gradually be processed in a similar manner. The synthetic data set obtained as described above (Fig. 17) was used as the basis for the authors' proposal for α_I.

A general power law functional relationship was adopted to capture the dependency on the imperfection amplitude δ_e/t (Eq. 9). This functional form has been widely used before to define the elastic imperfection reduction factor for cylinders under uniform axial compression in EN 1993-1-6 (2007), as well as by Chen *et al.* (2008) and Rotter (2013) to obtain the first trial expression for α_I for cylinders under uniform bending. It has the advantage that it is monotonically decreasing and conservatively predicts $\alpha_I \rightarrow 0$ as $\delta_e/t \rightarrow \infty$. Further, $\alpha_I = 1$ when $\delta_e/t = 0$, indicating perfect shell behaviour where $\alpha = \alpha_G$ only.

$$\alpha_I\left(L,\delta_e\right)=\frac{1}{1+x_1\left(\delta_e/t\right)^{x_2}} \text{ where } x_1, x_2 \text{ are } f\left(L\right) \tag{9}$$

The length-dependency of the physical relationship is achieved through the scaling parameters x_1 and x_2 that are allowed to vary with ω or Ω, depending on the length domain. A least-squares minimisation was first performed at every length ω or Ω to fit the expression for α_I (Eq. 9) to the synthetic imperfection sensitivity relationships (Figs 16 & 17), subject to the constraint that the fitted α_I expression cannot predict a higher buckling moment than that given by any of the data points. This resulted in sets of (x_1, x_2) pairs for different lengths and boundary conditions. A second, unconstrained, least-squares minimisation was then performed to fit convenient expressions to each of these x_1 or x_2 vs. length data sets (Fig. 18). This novel 'fit to a fit' procedure ensures that the design expression for α_I captures much of the physics of the underlying behaviour and predicts a realistic length-dependent imperfection sensitivity.

The proposed algebraic expressions for the x_1 and x_2 parameters, to be used together with the functional form for α_I in Eq. 9, are presented in Table 3 and illustrated in Fig. 18, while the moment-length relationship calculated on their basis is shown in Figs 19 and 20 (which the reader is invited to compare with Figs 17, 15 and then Figs 12 to 10, in that order). It is suggested that in fact only a single characterisation need be made of the x_1 and x_2 parameters in terms of ω so that it is valid for both BCr and BCf conditions within the 'medium' length domain, and similarly only one characterisation is necessary in terms of Ω within the 'transitional' and 'long' domains. The proposed expression for x_1 in the 'medium' domain tends to the same value of 1.7 as the starting value for x_1 in the 'transitional' domain as $\omega \rightarrow 0.5(r/t)$, thus ensuring continuity of the relationship across the length domain boundary, while for 'long' cylinders x_1 tends to an asymptotic value of 0.7 as $\Omega \rightarrow \infty$ representative of invariant imperfection sensitivity in (infinitely) 'long' cylinders. It was found that the x_2

parameter may be simply assigned a constant value of 0.7 at all lengths. The computed and fitted relationships between the buckling moment M_k / M_{cr} and the length illustrated in Figs 19 and 20 for varying δ_e/t should help the reader confirm that the characterisation is consistently conservative relative to both the BCr and BCf data.

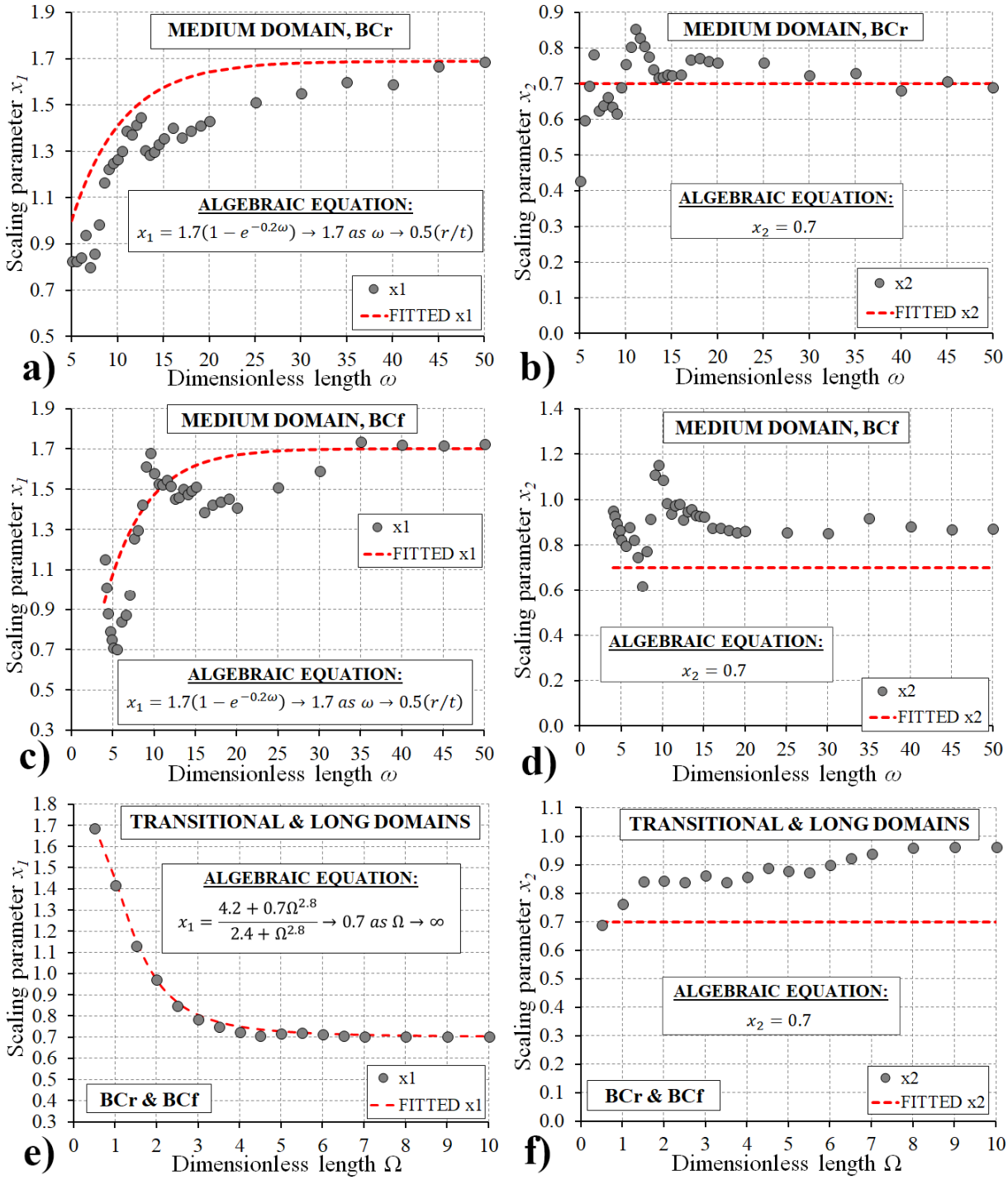

Fig. 18 – Construction of a fitted algebraic relationship between scaling parameters x_1 and x_2 and dimensionless lengths ω and Ω for both BCr and BCf end restraint conditions.

Table 3 – Proposed simple algebraic expressions for a length-dependent α_I parameter for imperfect elastic cylinders under uniform bending.

'Medium' **$5 < \omega \leq 0.5(r/t)$**	$x_1 = 1.7\left(1-e^{-0.2\omega}\right) \rightarrow 1.7$ as $\omega \rightarrow 0.5\left(\frac{r}{t}\right)$ $x_2 = 0.7$
'Transitional' & 'Long' **$\Omega \geq 0.5$**	$x_1 = \frac{4.2+0.7\Omega^{2.8}}{2.4+\Omega^{2.8}} \rightarrow \begin{cases} 1.7 \text{ as } \Omega \rightarrow 0.5 \\ 0.7 \text{ as } \Omega \rightarrow \infty \end{cases}$ $x_2 = 0.7$

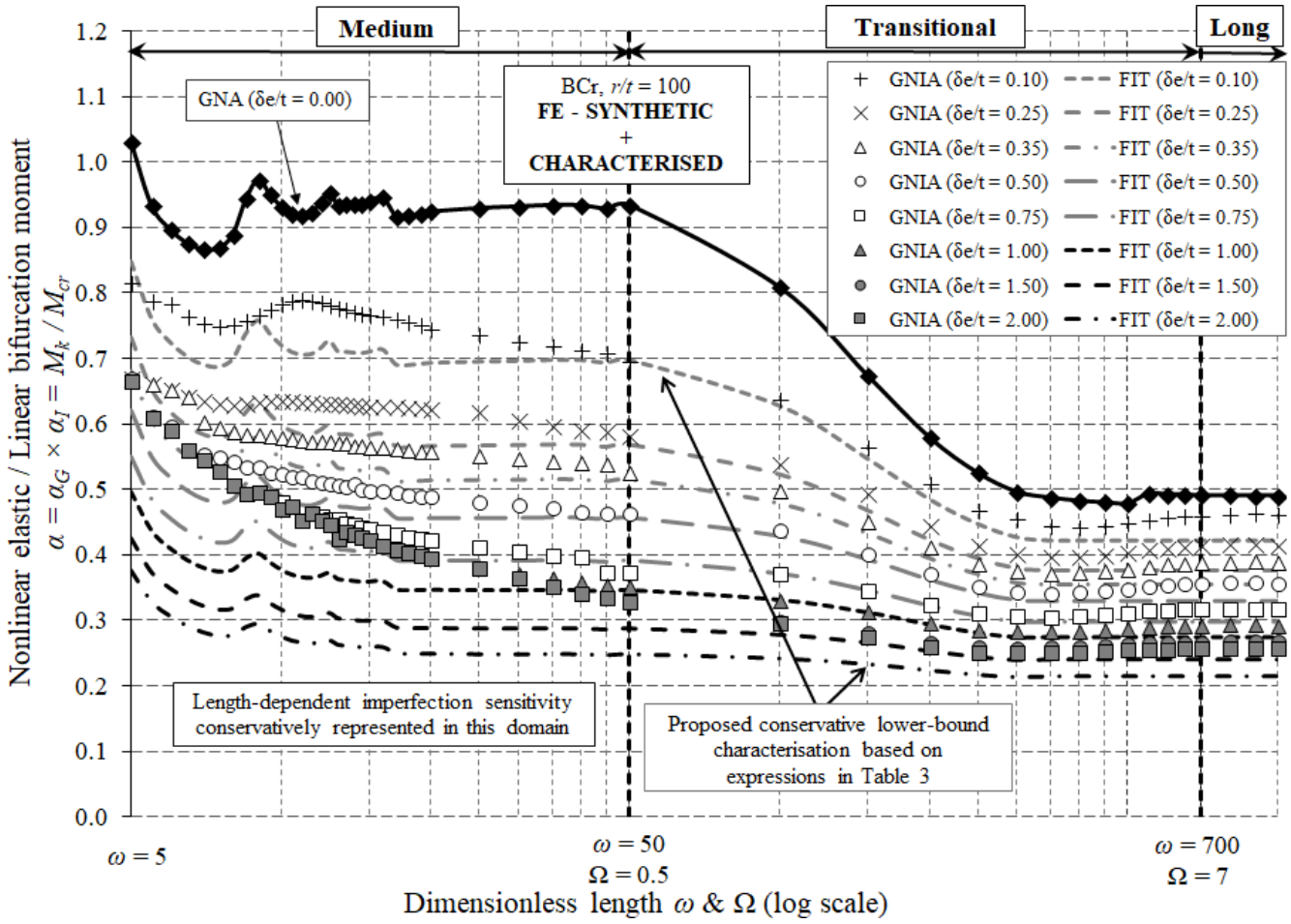

Fig. 19 – Resulting characterised relationship between M_k / M_{cr} and length for elastic imperfect cylinders under uniform bending with the BCr end restraint condition.

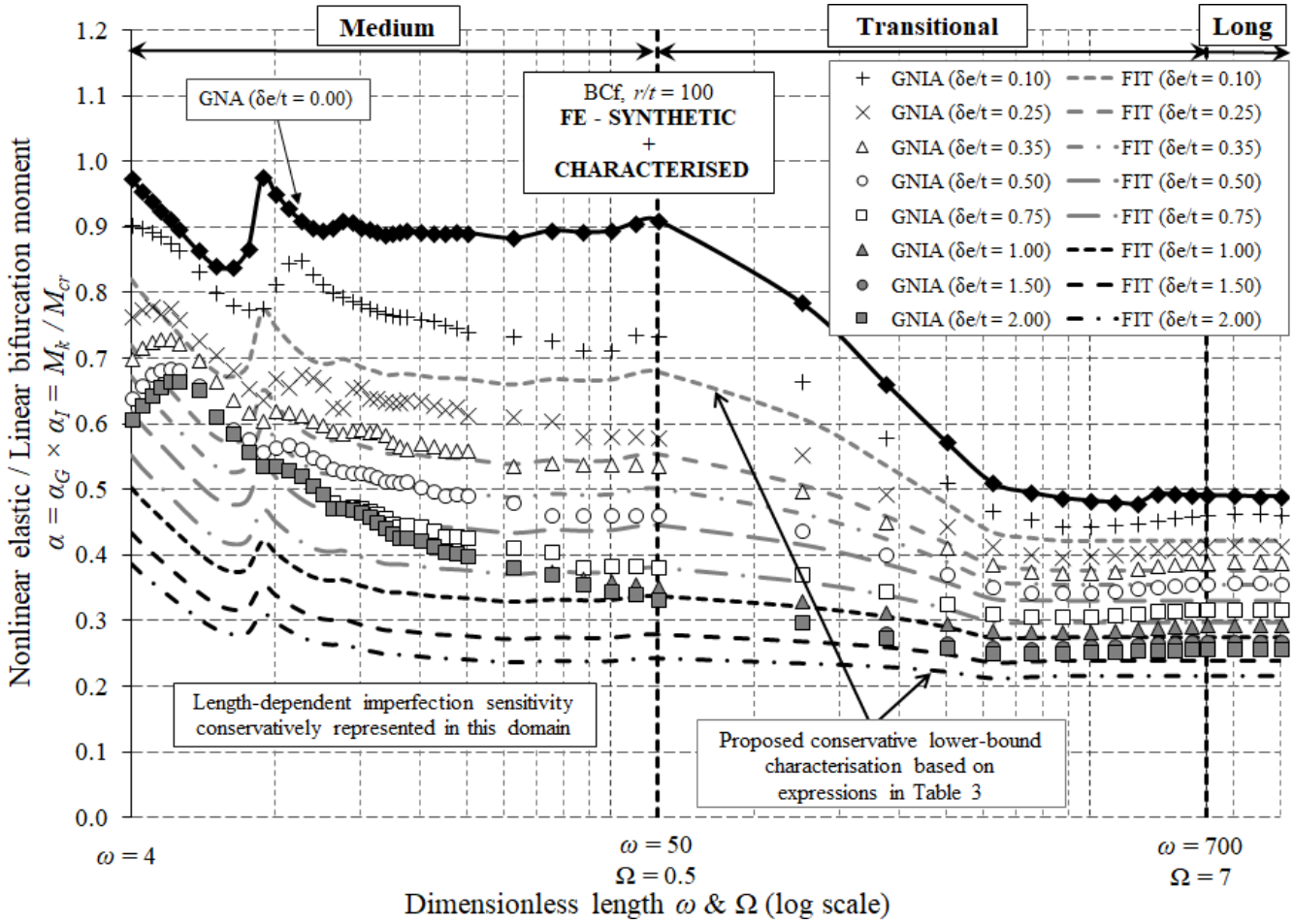

Fig. 20 – Resulting characterised relationship between M_k / M_{cr} and length for elastic imperfect cylinders under uniform bending with the BCf end restraint condition.

The authors take the liberty of suggesting, by way of a further simplification, that for design purposes the imperfection sensitivity in the 'medium' length domain (and perhaps even at all lengths) may be conservatively represented by α_I established at the 'most severe' length at the start of the 'transitional' domain, i.e. at $\Omega = 0.5$, such that $x_1 = 1.7$ and $x_2 = 0.7$ when $\omega \leq 0.5(r/t)$. This permits a simpler overall α_I expression represented by just *one* expression for each of the x_1 and x_2 parameters and dependent on Ω only. Lastly, cylinders with end boundary conditions that do not maintain rigidly circular ends should probably be treated as susceptible to fully-developed ovalisation at *all* lengths (Liu *et al.*, 2018), suggest an invariant reduction in buckling moment due to geometric nonlinearity of $\alpha_G \approx 0.5$ and an 'asymptotic' imperfection sensitivity such that $x_1 = x_2 = 0.7$ (i.e. *not* the most severe).

8. Conclusions

This paper has presented an exhaustive computational study into the imperfection sensitivity of cylindrical shells under uniform bending, covering a wide parametric variation of cylinder length, end support conditions, forms and amplitudes of geometric imperfections. The following key conclusions may be drawn:

- Imperfection sensitivity is strongly length-dependent, with the most severe sensitivity predicted for cylinders at a length where ovalisation is just beginning to influence the pre-buckling behaviour. Very long cylinders dominated by fully-developed pre-buckling ovalisation are significantly less sensitive to geometric imperfections.
- The system exhibits an imperfection sensitivity that does not necessarily suggest a monotonically decreasing buckling moment with growing imperfection amplitude. This is especially the case for shorter cylinders where the end boundary condition may be very effective in constraining larger buckles characteristic of more imperfect cylinders.
- Of the three imperfection forms considered (eigenmode, imposed ovalisation and weld depression), the axisymmetric circumferential Type 'A' weld depression of Rotter & Teng appears to be the most deleterious to the strength of the cylinder at all lengths, in addition to being a realistic model of typical defects found in many cylindrical shells in service. It is recommended as an optimal form for similar explorations in other shell systems governed by significant pre-buckling meridional compression.
- Conservative but realistic and closed-form algebraic design expressions were formulated to describe the reduction in buckling moment due to the effect of imperfections. The proposed relationships are dependent on the cylinder length, the *r/t* ratio and imperfection amplitude, and are intended for implementation within the Reference Resistance Design framework recently adopted by EN 1993-1-6.
- This study appears to be the first to systematically document the length-dependency of imperfection sensitivity in *any* shell system. The authors encourage the shell buckling research community to explore the imperfection sensitivity of other systems, even very classical and otherwise well-studied ones, for a similarly strong dependency on a global geometric parameter such as, in the case of cylinders, the length. This paper employed a novel automation strategy designed to facilitate this task.

Acknowledgements

This work was funded by the Petroleum Technology Development Fund (PTDF) of Nigeria. The authors are very grateful to Professor J. Michael Rotter for the numerous and pleasant joint discussions on this and other topics, and warmly dedicate this paper to the Special Issue of Advances in Structural Engineering in honour of his 70th birthday and a lifetime of achievements in shell buckling and Standards development.

References

ABAQUS (2014) *ABAQUS version 6.14*. Dassault Systèmes Simulia Corp., Providence, RI, USA.

Aksel'rad E. & Emmerling F. (1984) *Collapse load of elastic tubes under bending*. Israel Journal of Technology, 22, 85.

Berry P.A., Rotter J.M. & Bridge R.Q. (2000) *Compression tests on cylinders with circumferential weld depressions*. Journal of Engineering Mechanics, 126 (4), 405-413.

Brazier L.G. (1927) *On the flexure of thin cylindrical shells and other thin sections*. Proceedings of the Royal Society A, 116 (773), 104-114.

Bushnell D. (1985) *Computerized buckling analysis of shells*. Martinus Nijhoff Publishers, Dordrecht, The Netherlands, Dordrecht, The Netherlands.

Calladine C. R. (1983) *Theory of shell structures*. University Press, Cambridge.

Chapelle D. & Bathe K. (2010) *The Finite Element Analysis of Shells - Fundamentals*. 2nd edition. Springer, London.

Chen L., Doerich C. & Rotter J.M. (2008) *A study of cylindrical shells under global bending in the elastic-plastic range*. Steel Construction, 1 (1), 59-65.

EN 1993-1-6. (2007) *Eurocode 3: Design of steel structures. Part 1-6: strength and stability of shell structures*. European Committee for Standardization (CEN), Brussels.

Fajuyitan O. K., Sadowski A. J. & Rotter J. M. (2015) *A study of imperfect cylindrical steel tubes under global bending and varying support conditions*. Proceedings of the 8th International Conference on Advances in Steel Structures, July 21 - 24, Lisbon, Portugal.

Fajuyitan O.K., Sadowski A.J. & Wadee M.A. (2017) *Buckling of very short elastic cylinders with weld imperfections under uniform bending*. Steel Construction, 10 (3), 216-221.

Fajuyitan O.K., Sadowski A.J., Wadee M.A. & Rotter J.M. (2018) *Nonlinear behaviour of short elastic cylindrical shells under global bending*. Thin-Walled Structures, 124, 574-587.

Guarracino F. (2003) *On the analysis of cylindrical tubes under flexure: theoretical formulations, experimental data and finite element analyses*. Thin-Walled Structures, 41 (2), 127-147.

Hutchinson J.W. & Koiter W.T. (1970) *Postbuckling theory*. Applied Mechanics Reviews, 23, 1353-1366.

Karamanos, S.A. (2002) *Bending instabilities of elastic tubes. International Journal of Solids and Structures*, 39 (8), 2059-2085.

Koiter W. T. (1945) *On the stability of elastic equilibrium*. PhD Thesis. Delft University (in Dutch).

Koiter W. T. (1963) *The effect of axisymmetric imperfections on the buckling of cylindrical shells under axial compression*. Proc. K. Ned. Akad. Wet., Ser. B: Phys. Sci, .

Li L. & Kettle R. (2002) *Nonlinear bending response and buckling of ring-stiffened cylindrical shells under pure bending*. International Journal of Solids and Structures, 39 (3), 765-781.

Liu Q., Sadowski A.J. & Rotter J.M. (2018) *Ovalization restraint in four-point bending tests of tubes*. Under review.

MATLAB. (2014) *MATLAB version 8.4 (R2014b)*. The MathWorks Inc., Natick, MA.

Pircher M., Berry P.A., Ding X. & Bridge R.Q. (2001) *The shape of circumferential weld-induced imperfections in thin-walled steel silos and tanks*. Thin-Walled Structures, 39 (12), 999-1014.

Reissner E. (1961) *On finite pure bending of cylindrical tubes*. Österreichisches Ingenieur -- Archive, 15 (1-4), 165-172.

Riks E. (1979) *An incremental approach to the solution of snapping and buckling problems*. International Journal of Solids and Structures, 15 (7), 529-551.

Rotter J. M. (2004) *Cylindrical shells under axial compression*. In: Buckling of thin metal shells, London.42-87.

Rotter J. M. (2007) *A framework for exploiting different computational assessments in structural design*. Proceedings of the 6th international conference on steel and aluminium structures, July, 2007, Oxford, UK.

Rotter J.M. (2013) *New segment in Annex E of EN 1993-1-6 on cylindrical shells under global bending and spherical shells under external pressure*. Amendment AM-1-6-2013-13 to EN 1993-1-6 approved by CEN/TC250/SC3, November 2013, Zürich, Switzerland.

Rotter J. M. (2016a) *The new method of reference resistance design for shell structures*. Proc. SDSS 2016, Int. Colloq. On stability & ductility of Steel Structures, Timisoara, Romania.

Rotter J. M. (2016b) *Advances in understanding shell buckling phenomena and their characterisation for practical design*. In: Recent Progress in Steel and Composite Structures: Proceedings of the XIII International Conference on Metal Structures (ICMS2016, Zielona Góra, Poland, 15-17 June 2016), London.3-16.

Rotter J.M. (2016c) *Buckling of cylindrical shells under axial compression: imperfection sensitivity, tolerances and computational strength assessments*. In Preparation.

Rotter J.M., Sadowski A.J. & Chen L. (2014) *Nonlinear stability of thin elastic cylinders of different length under global bending*. International Journal of Solids and Structures, 51 (15–16), 2826-2839.

Rotter J.M. & Teng J.G. (1989) *Elastic stability of cylindrical shells with weld depressions*. Journal of Structural Engineering, 115 (5), 1244-1263.

Rotter J.M. & Al-Lawati (2016) *Length effects in the buckling of imperfect axially-compressed cylinders*. Proc. SDSS 2016, Int. Colloq. On stability & ductility of Steel Structures, Timisoara, Romania.

Sadowski A.J. & Rotter, J.M. (2011a) *Buckling of very slender metal silos under eccentric discharge*. Engineering Structures, 33 (4), 1187-1194.

Sadowski A.J. & Rotter J.M. (2011b) *Steel silos with different aspect ratios: II – behaviour under eccentric discharge*. Journal of Constructional Steel Research, 67, 1545-1553.

Sadowski A.J. & Rotter J.M. (2012) *Structural behaviour of thin-walled metal silos subject to different flow channel sizes under eccentric discharge pressures*. ASCE Journal of Structural Engineering, 7(1), 922-931.

Sadowski A.J. & Rotter J.M. (2013a) *Solid or shell finite elements to model thick cylindrical tubes and shells under global bending*. International Journal of Mechanical Sciences, 74, 143-153.

Sadowski A.J. & Rotter J.M. (2013b) *Exploration of novel geometric imperfection forms in buckling failures of thin-walled metal silos under eccentric discharge*. International Journal of Solids and Structures, 50, 781-794.

Sadowski A.J., Fajuyitan O.K. & Wang, J. (2017) *A computational strategy to establish algebraic parameters for the Reference Resistance Design of metal shell structures*. Advances in Engineering Software, 109, 15-30.

Seide P. & Weingarten V.I. (1961) *On the buckling of circular cylindrical shells under pure bending*. Journal of Applied Mechanics, 28 (1), 112-116.

Song C.Y., Teng J.G. & Rotter J.M. (2004) *Imperfection sensitivity of thin elastic cylindrical shells subject to partial axial compression*. International Journal of Solids and Structures, 41 (24–25), 7155-7180.

Stephens W.B., Starnes J.H. & Almroth B.O. (1975) *Collapse of long cylindrical shells under combined bending and pressure loads*. AIAA Journal, 13 (1), 20-25.

Tatting B., Gürdal Z. & Vasiliev V. (1997) *The Brazier effect for finite length composite cylinders under bending*. International Journal of Solids and Structures, 34 (12), 1419-1440.

Thompson J. M. T. & Hunt G. W. (1973) *A general theory of elastic stability*. John Wiley & Sons Ltd, London.

Thompson J. M. T. & Hunt G. W. (1984) *Elastic instability phenomena*. John Wiley & Sons, Chichester

Vasilikis D., Karamanos S., van Es S.H.J. & Gresnigt A.M.N. (2016) *Ultimate bending capacity of spiral-welded steel tubes – Part II: Predictions*. Thin-Walled Structures, 102, 305-319.

Wang J., Fajuyitan O.K., Sadowski A.J. & Rotter J.M. (2018) *A comprehensive characterisation of cylindrical shells under uniform bending in the framework of Reference Resistance Design*. In Preparation.

Wood J. (1958) *The flexure of a uniformly pressurized, circular, cylindrical shell*. Journal of Applied Mechanics, 25 (12), 453-458.

Xu Z., Gardner L. & Sadowski A.J. (2017) *Nonlinear stability of elastic elliptical cylindrical shells under uniform bending*. International Journal of Mechanical Sciences, 128, 593-606.

Yamaki, N (1984) *Elastic stability of circular cylindrical shells*. Elsevier Science, North-Holland.